the basis function for tungsten, the exponents for the 6s and 6p orbitals were both fixed at 1.80. All calculations were converged with a self-consistent-field iterative technique using a convergence criteria of 0.0010 as the largest deviation of atomic orbital populations between successive cycles.

Acknowledgment. We thank the National Science Foundation for financial support. R.H.C. is a National Science Foundation Postdoctoral Fellow.

Registry No. 1, 137122-24-8.

Supplementary Material Available: Listings of anisotropic thermal parameters and all bond distances and angles and VERSORT drawings (8 pages); a listing of F_o and F_c (6 pages). Ordering information is given on any current masthead page.

Organometallic Oxides: Preparation and Properties of the Diamagnetic Trinuclear Cluster $\{[(\eta\text{-}C_5Me_5)Nb(\mu\text{-}Cl)(\mu\text{-}O)]_3\}^+$ and Related Chloride–Oxides of Niobium

Frank Bottomley* and Selami Karslioglu†

Department of Chemistry, University of New Brunswick, Fredericton, New Brunswick, Canada E3B 5A3

Received July 1, 1991

Oxidation of $(\eta\text{-}C_5Me_5)_2NbCl_2$ with O_2 in tetrahydrofuran containing traces of water gave $[(\eta\text{-}C_5Me_5)NbCl_2]_2(\mu\text{-}Cl)(\mu\text{-}OH)(\mu\text{-}O)$ (**1**) and polymeric $[Nb_2Cl_2O_4(thf)_3]_n$. Complex **1** (for which a newly refined structure is reported) existed as two isomers, which are distinguished by the relative orientation of $\eta\text{-}C_5Me_5$ and the bridging ligands. Reduction of **1** with zinc powder gave $\{[(\eta\text{-}C_5Me_5)Nb(\mu\text{-}Cl)(\mu\text{-}O)]_3\}^+$ (**2**$^+$), which was isolated in combination with three different anions: $\{[ZnCl_2(\mu\text{-}Cl)]_2\}^{2-}$, $\{[ZnCl]_4(\mu\text{-}Cl)_6\}^{2-}$, and $(\{[ZnCl]_6(\mu\text{-}Cl)_8\}^{2-})_n$. Cluster **2**$^+$ contained Nb_3^{13+}, was diamagnetic, and had an equilateral triangle of Nb atoms (average Nb–Nb distance 2.876 (1) Å), each edge of which was bridged by Cl and O atoms (average Nb–Cl = 2.542 (1) Å, average Nb–O 1.937 (3) Å). The geometry and electronic structure of **2**$^+$ are compared with those of $\{[(\eta\text{-}C_5Me_5)Re(\mu\text{-}O)_2]_3\}^{2+}$ and $\{[(\eta\text{-}C_6Me_6)Nb(\mu\text{-}Cl)_2]_3\}^{n+}$ ($n = 1, 2$). The structure of the $Zn_4Cl_{10}{}^{2-}$ salt of **2**$^+$ was reported previously. The $Zn_2Cl_6{}^{2-}$ salt was monoclinic, space group $A2/m$, $a = 14.7497$ (8) Å, $b = 16.311$ (2) Å, $c = 16.410$ (2) Å, $\beta = 95.67$ (1)°, $Z = 2$ (of $\{\mathbf{2}\}_2\{Zn_2Cl_6\}\cdot C_6H_{14}$), and $R = 0.040$. The $Zn_6Cl_{14}{}^{2-}$ salt was triclinic, $P\bar{1}$, $a = 11.141$ (4) Å, $b = 14.793$ (7) Å, $c = 14.792$ (5) Å, $\alpha = 74.14$ (4)°, $\beta = 77.40$ (3)°, $\gamma = 77.32$ (4)°, $Z = 2$ (of $\{\mathbf{2}\}\{Zn_3Cl_7\}$), and $R = 0.104$. Oxidation of the salts of **2**$^+$ in CH_2Cl_2 solution with O_2 gave $\{[(\eta\text{-}C_5Me_5)NbCl]_3(\mu\text{-}Cl)(\mu\text{-}O)_2(\mu_3\text{-}OH)(\mu_3\text{-}O)\}^+$ (**3**$^+$), isolated as the $\{[ZnCl_2(\mu\text{-}Cl)]_2\}^{2-}$ salt. Cluster **3**$^+$ had an isosceles triangle of Nb atoms (Nb–Nb = 3.028 (2) Å (×2) and 3.318 (2) Å). The long Nb–Nb edge was bridged by Cl. The μ_3-O ligand had much shorter distances to the two Nb atoms forming the long edge (average 2.046 (8) Å) than to the third Nb (2.228 (8) Å). The μ_3-OH ligand had equal distances to all three Nb atoms (average 2.207 (8) Å). The salt $\{\mathbf{3}\}_2\{Zn_2Cl_6\}$ was monoclinic, $P2_1/a$, $a = 11.377$ (1) Å, $b = 30.630$ (2) Å, $c = 11.442$ (1) Å, $\beta = 100.82$ (1)°, $Z = 4$ (of $\{\mathbf{3}\}\{ZnCl_3\}$), and $R = 0.070$. The physical and chemical properties of **2**$^+$ and **3**$^+$ are reported and compared to those of related compounds.

Introduction

We have been synthesizing (cyclopentadienyl)metal oxides by two methods: oxidative aggregation of low-valent (cyclopentadienyl)metal derivatives (for example the preparation of $[(\eta\text{-}C_5Me_5)Cr(\mu_3\text{-}O)]_4$ by oxidation of $(\eta\text{-}C_5Me_5)_2Cr$ with N_2O[1]); reductive aggregation of high-valent (cyclopentadienyl)metal oxo complexes (for example the preparation of $\{[(\eta\text{-}C_5H_5)MoCl]_4(\mu\text{-}O)_6\}\{ZnCl(thf)\}_2$ by reduction of $(\eta\text{-}C_5H_5)MoCl_2(O)$ with zinc powder[2]). We have also reported recently the preparation of the trinuclear oxide $[(\eta\text{-}C_5H_5)NbCl(\mu\text{-}Cl)]_3(\mu_3\text{-}OH)(\mu_3\text{-}O)$[3] by the reduction of $[(\eta\text{-}C_5H_5)NbCl_3(H_2O)]_2(\mu\text{-}O)$[4-7] with aluminum powder.[8] Attempts to reduce $[(\eta\text{-}C_5H_5)NbCl(\mu\text{-}Cl)]_3(\mu_3\text{-}OH)(\mu_3\text{-}O)$ further (our goal being $[(\eta\text{-}C_5H_5)Nb]_5(\mu_3\text{-}O)_6$, which would be the niobium analogue of $[(\eta\text{-}C_5H_5)V]_5(\mu_3\text{-}O)_6$[9]) gave only intractable products. Therefore, we have turned to the $\eta\text{-}C_5Me_5$ derivatives of niobium. As with the $\eta\text{-}C_5H_5$ complexes, suitable starting materials for either oxidative or reductive aggregation are not readily available. Of the obvious choices for oxidative aggregation, neither $(\eta\text{-}C_5Me_5)_2Nb$ nor $(\eta\text{-}C_5Me_5)Nb(CO)_4$ is known, although the tantalum analogue of the latter has been prepared.[10,11] The obvious choice for reductive aggregation is $(\eta\text{-}C_5Me_5)NbCl_2(O)$, the vanadium analogue of which has been investigated extensively.[12-16] However, this too is

---

* To whom correspondence should be addressed.

† Permanent address: Department of Chemistry, Karadeniz Technical University, Trabzon, Turkey.

(1) Bottomley, F.; Chen, J.; MacIntosh, S. M.; Thompson, R. C. *Organometallics* **1991**, *10*, 906.

(2) Bottomley, F.; Ferris, E. C.; White, P. S. *Organometallics* **1990**, *9*, 1166.

(3) Curtis, M. D.; Real, J. *Inorg. Chem.* **1988**, *27*, 3176.

(4) Daran, J.-C.; Prout, K.; De Cian, A.; Green, M. L. H.; Siganporia, N. *J. Organomet. Chem.* **1977**, *136*, C4.

(5) Prout, K.; Daran, J.-C. *Acta Crystallogr.* **1979**, *B35*, 2882.

(6) Andreu, A. M.; Jalón, F. A.; Otero, A.; Royo, P.; Lanfredi, A. M. M.; Tiripicchio, A. *J. Chem. Soc., Dalton Trans.* **1987**, 953.

(7) Jalón, F. A.; Otero, A.; Royo, P.; Fernandez-G., J. M.; Rosales, M. J.; Toscano, R. A. *J. Organomet. Chem.* **1987**, *331*, C1.

(8) Bottomley, F.; Keizer, P. N.; White, P. S.; Preston, K. F. *Organometallics* **1990**, *9*, 1916.

(9) Bottomley, F.; Paez, D. E.; White, P. S. *J. Am. Chem. Soc.* **1983**, *104*, 5651.

(10) Gibson, V. C.; Kee, T. P.; Clegg, W. *J. Chem. Soc., Dalton Trans.* **1990**, 3199.

(11) Herrmann, W. A.; Kalcher, W.; Biersack, H.; Bernal, I.; Creswick, M. *Chem. Ber.* **1981**, *114*, 3558.

(12) Bottomley, F.; Darkwa, J.; Sutin, L. C.; White, P. S. *Organometallics* **1986**, *5*, 2165.

(13) Bottomley, F.; Sutin, L. C. *J. Chem. Soc., Chem. Commun.* **1987**, 1112.

0276-7333/92/2311-0326$03.00/0

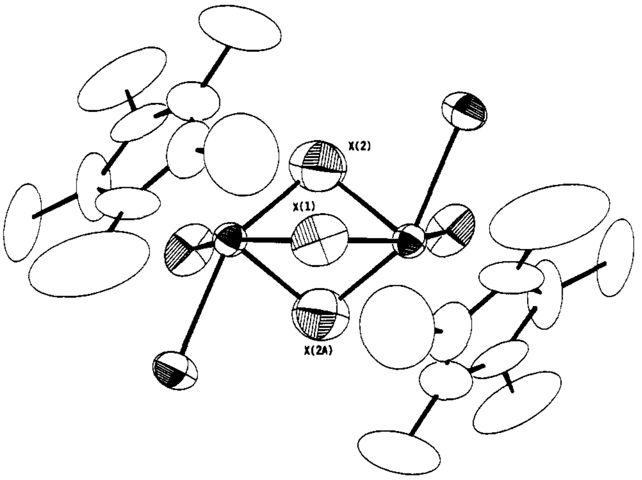

Figure 1. Structure of $[(\eta\text{-}C_5Me_5)NbCl_2]_2(\mu\text{-}Cl)(\mu\text{-}OH)(\mu\text{-}O)$ (1).

unknown, although a dimeric form of the tantalum analogue $[(\eta\text{-}C_5Me_5)TaCl_2(\mu\text{-}O)]_2$ has been obtained.[17]

The hydrolysis of $(\eta\text{-}C_5R_5)MCl_4$ (M = Nb, Ta; R = H, Me) has been discussed by several groups.[4-8,18-25] It leads to a complicated mixture of products, most of which are dinuclear (for example $[(\eta\text{-}C_5Me_5)TaCl_2(OH)]_2(\mu\text{-}O)$[19] and $[(\eta\text{-}C_5H_4SiMe_3)NbCl_2]_2(\mu\text{-}Cl)_2(\mu\text{-}O)$[6]) or trinuclear (for example $[(\eta\text{-}C_5Me_5)MCl]_3(\mu\text{-}Cl)(\mu\text{-}O)_3(\mu_3\text{-}O)$ (M = Nb,[23,25] Ta[19,24])). The product that is formed depends on the experimental conditions. The yields of any particular product are relatively low, and separation of the products is not trivial. In the case of tantalum the conditions of hydrolysis can be engineered to give a high yield of $[(\eta\text{-}C_5Me_5)TaCl_2(OH)]_2(\mu\text{-}O)$,[19] but no reliable route to a niobium complex containing a reasonable amount of oxygen has been found. We therefore sought an alternative route to $(\eta\text{-}C_5Me_5)NbCl_2(O)$ or to any other chloro–oxo derivative of $(\eta\text{-}C_5Me_5)Nb$ which could be obtained in reasonable yield and was suitable for reductive aggregation to (pentamethylcyclopentadienyl)niobium oxides. We describe here the preparation of $[(\eta\text{-}C_5Me_5)NbCl_2]_2(\mu\text{-}Cl)(\mu\text{-}OH)(\mu\text{-}O)$ (1) by oxidation of $(\eta\text{-}C_5Me_5)_2NbCl_2$ with O_2 in a tetrahydrofuran solution containing traces of water. Reduction of 1 with zinc powder gave the novel trinuclear oxide $\{[(\eta\text{-}C_5Me_5)Nb(\mu\text{-}Cl)(\mu\text{-}O)]_3\}^+$ (2^+). Reoxidation of 2^+ with O_2 gave $\{[(\eta\text{-}C_5Me_5)NbCl]_3(\mu\text{-}Cl)(\mu\text{-}O)_2(\mu_3\text{-}OH)(\mu_3\text{-}O)\}^+$ (3^+). The physical and chemical properties of 1, 2^+, and 3^+ are discussed, as are the structures of the chlorozincate anions $\{[ZnCl_2(\mu\text{-}Cl)]_2{}^{2-}$, $\{[ZnCl]_4(\mu\text{-}Cl)_6\}^{2-}$, and $(\{[ZnCl]_6(\mu\text{-}Cl)_8\}^{2-})_n$, which form the anions to 2^+ and 3^+.

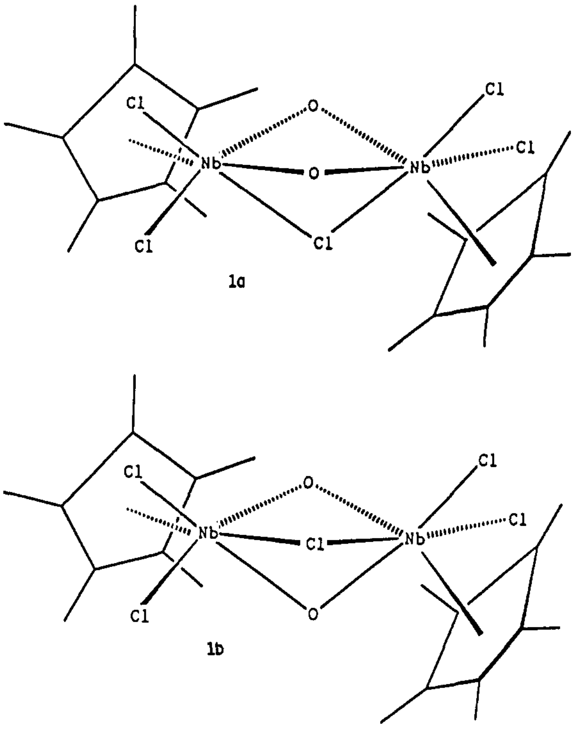

Figure 2. Two isomers of $[(\eta\text{-}C_5Me_5)NbCl_2]_2(\mu\text{-}Cl)(\mu\text{-}OH)(\mu\text{-}O)$: **1a**, C_2 isomer; **1b**, C_1 isomer.

A brief account of part of this work has appeared.[26]

Results and Discussion

Preparation of $[(\eta\text{-}C_5Me_5)NbCl_2]_2(\mu\text{-}Cl)(\mu\text{-}OH)(\mu\text{-}O)$ (1). When a solution of $(\eta\text{-}C_5Me_5)_2NbCl_2$[21] in tetrahydrofuran (thf) was oxidized with O_2, a mixture of orange 1 (see Figures 1 and 2) and a purple compound was formed. On removal of the solvent and extraction of the residue with toluene, the purple compound dissolved, leaving insoluble, orange-red 1, which was recrystallized from CH_2Cl_2/ether in 50% yield (based on niobium). The purple compound could be precipitated from the toluene solution by the addition of hexane. However, only a portion of it would redissolve in toluene, and the soluble portion decreased in quantity with each precipitation and dissolution. Microanalysis and spectroscopy suggested that the purple compound had the approximate formula $Nb_2Cl_2O_4(thf)_3$. It did not contain C_5Me_5, and its properties were consistent with it being a polymer. Therefore, it was not investigated further.

Compound 1 contains an OH group, and therefore a source of protons is necessary for its formation. When the thf solvent used in the oxidation of $(\eta\text{-}C_5Me_5)_2NbCl_2$ by O_2 was rigorously dried, the proportion of 1 in the product decreased. However, some 1 was always obtained, even under the most stringently anhydrous conditions. Addition of a few drops of water to the thf solution before oxidation markedly increased the proportion of 1, but a large excess of water (such as in present in commercial thf without predrying) gave a mixture of products, presumably because of hydrolysis of 1 and/or $(\eta\text{-}C_5Me_5)_2NbCl_2$. Assuming that the source of protons is water, the oxidation can be represented by eq 1. The maximum yield of 1 is 67% based on the niobium in $(\eta\text{-}C_5Me_5)_2NbCl_2$.

$$12(\eta\text{-}C_5Me_5)_2NbCl_2 + 7O_2 + 2H_2O + 6\text{thf} \rightarrow 4\ \mathbf{1} + 2Nb_2Cl_2O_4(\text{thf})_3 + 8(C_5Me_5)_2 \quad (1)$$

---

[14] Bottomley, F.; Magill, C. P.; Zhao, B. *Organometallics* **1990**, *9*, 1700.

[15] Herrmann, W. A.; Weichselbaumer, G.; Kneuper, H.-J. *J. Organomet. Chem.* **1987**, *319*, C21.

[16] Herberhold, M.; Kremnitz, W.; Kuhnlein, M.; Ziegler, M. L.; Brunn, K. *Z. Naturforsch.* **1987**, *42B*, 1520.

[17] Gibson, V. C.; Kee, T. P. *J. Chem. Soc., Chem. Commun.* **1989**, 656.

[18] Bunker, M. J.; De Cian, A.; Green, M. L. H.; Moreau, J. J. E.; Siganporia, N. *J. Chem. Soc., Dalton Trans.* **1980**, 2155.

[19] Jernakoff, P.; de Méric de Bellefon, C.; Geoffroy, G. L.; Rheingold, A. L.; Geib, S. J. *New J. Chem.* **1988**, *12*, 329.

[20] Arnold, J.; Shina, D. N.; Tilley, T. D.; Arif, A. M. *Organometallics* **1986**, *5*, 2037.

[21] Bunker, M. J.; DeCian, A.; Green, M. L. H. *J. Chem. Soc., Chem. Commun.* **1977**, 56.

[22] Gibson, V. C.; Kee, T. P.; Clegg, W. *J. Chem. Soc., Chem. Commun.* **1990**, 29.

[23] De la Mata, J.; Fardos, R.; Gômez, M.; Gômez-Sal, P.; Martinez-Carrera, S.; Royo, P. *Organometallics* **1990**, *9*, 2846.

[24] Jernakoff, P.; de Meric de Bellefon, C.; Geoffroy, G. L.; Rheingold, A. L.; Geib, S. J. *Organometallics* **1987**, *6*, 1362.

[25] Leichtweis, I.; Roesky, H. W.; Noltemeyer, M.; Schmidt, H.-G. *Chem. Ber.* **1991**, *124*, 253.

[26] Bottomley, F.; Karslioglu, S. *J. Chem. Soc., Chem. Commun.* **1991**, 222.

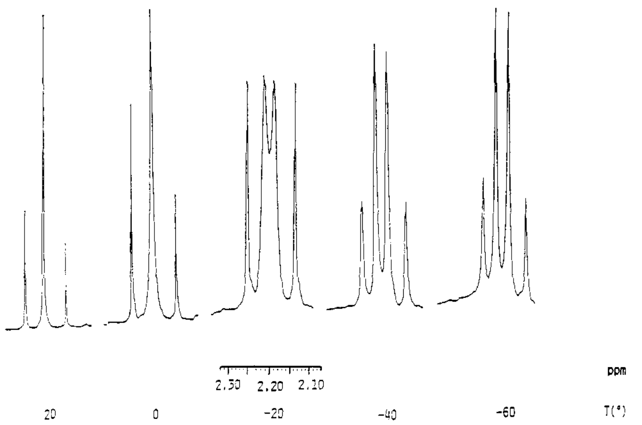

Figure 3. ^{1}H NMR spectrum of 1.

Compound 1 is related to $[(\eta\text{-}C_5H_4SiMe_3)NbCl_2]_2(\mu\text{-}Cl)_2(\mu\text{-}O)$, prepared by hydrolysis of $(\eta\text{-}C_5H_4SiMe_3)NbCl_4$.[6] Formation of $[(\eta\text{-}C_5Me_5)NbCl_2]_2(\mu\text{-}Cl)_2(\mu\text{-}O)$ on oxidation of $(\eta\text{-}C_5Me_5)_2NbCl_2$ would not require a source of protons but would require extra chlorine. This could only come by producing Nb_2O_5, for example by eq 2. This is thermodynamically very unfavorable in thf solution. On the scale of the experiments conducted in the present work, 70 ppm of H_2O would be sufficient to provide all of the protons required by eq 1. We believe that extraneous water, either in the thf solvent, in the O_2 gas, or adsorbed on the glassware, is the source of protons.

$$12(\eta\text{-}C_5Me_5)_2NbCl_2 + 7O_2 \rightarrow 4[(\eta\text{-}C_5Me_5)NbCl_2]_2(\mu\text{-}Cl)_2(\mu\text{-}O) + 2Nb_2O_5 + 8(C_5Me_5)_2 \quad (2)$$

Any synthesis with a maximum yield of 67% is not ideal. However, the preparation of 1 by oxidation of $(\eta\text{-}C_5Me_5)_2NbCl_2$ with O_2 does overcome many of the problems of the hydrolysis routes to (pentamethylcyclopentadienyl)niobium chloride oxide complexes. Compound 1 was readily separated and purified, there being no other product containing an $\eta\text{-}C_5Me_5$ ligand. The preparation of 1 was reproducible and not markedly dependent on the experimental conditions.

Structure of $[(\eta\text{-}C_5Me_5)_2NbCl_2]_2(\mu\text{-}Cl)(\mu\text{-}OH)(\mu\text{-}O)$ (1). As noted above, complex 1 is related to $[(\eta\text{-}C_5H_4SiMe_3)NbCl_2]_2(\mu\text{-}Cl)_2(\mu\text{-}O)$[6] and also to $[(\eta\text{-}C_5H_4SiMe_3)NbCl]_2(\mu\text{-}\eta^2\text{-}o\text{-}C_6H_4O)_2(\mu\text{-}O)$.[7] In any complex of type $[(\eta\text{-}C_5R_5)MX_2]_2(\mu\text{-}A)_2(\mu\text{-}B)$ two isomers are possible. These are shown for 1 in Figure 2. Note that the location of the hydrogen atom of 1 shown in Figure 2 is arbitrary. It may be located on either oxygen or symmetrically placed between them. Its position does not affect the existence of isomers, because **1a** and **1b** are distinguished by the relative positions of the $\eta\text{-}C_5Me_5$ and the bridging Cl ligands. The complex $[(\eta\text{-}C_5H_4SiMe_3)NbCl_2]_2(\mu\text{-}Cl)_2(\mu\text{-}O)$ has the structure represented by isomer **1b**. In the crystal of 1 there is disorder between the bridging groups. The disorder is due to the presence of both **1a** and **1b** in the crystal. The presence of the two isomers is shown clearly by the ^{1}H NMR spectrum of 1, which is illustrated in Figure 3. This spectrum is of a sample of 1 from which a crystal was selected for X-ray diffraction experiments; the spectrum was reproducible, although the relative intensities of the A and B portions of the spectrum differed from sample to sample. At 20 °C there were three resonances, at 2.24, 2.20, and 2.13 ppm, with an intensity ratio of 1:3:1. These are due to the CH_3 protons of the $\eta\text{-}C_5(CH_3)_5$ ligands. We assign the resonance at 2.20 ppm to the isomer **1a** (which has C_2 symmetry with equivalent $\eta\text{-}C_5Me_5$ ligands) and the other two resonances to the isomer **1b** (which has C_1 symmetry and inequivalent $\eta\text{-}C_5Me_5$ ligands). On cooling of the sample to −60 °C, the signal at 2.20 ppm due to isomer **1a** split into two signals of equal intensity, whereas the signals due to isomer **1b** remained unchanged. We believe that the splitting in the signal from the symmetrical isomer **1a** is due to localization of the proton on one or the other of the bridging oxygen atoms.

The ^{1}H NMR spectra of different samples of 1 at room temperature always showed the three resonances shown in Figure 3, and the resonances at 2.24 and 2.13 ppm always had the same relative intensity. However, the ratio of the intensity of the resonances at 2.24 and 2.13 ppm to that at 2.20 ppm varied. This must be due to varying amounts of the isomers **1a** and **1b** being formed in the reaction between $(\eta\text{-}C_5Me_5)_2NbCl_2$ and O_2. Once formed, the isomers **1a** and **1b** must interconvert only very slowly, if at all, because of the rigidity of the triply bridged core of 1. A caveat to this interpretation needs to be made on the basis of the molecular weight of 1 as determined by osmometry in $CHCl_3$ solution. This was 940, compared to a calculated value of 666. This indicated that association of 1 occurred. Such association must involve the breaking of the intramolecular Nb–(μ-OH)–Nb and/or Nb–(μ-Cl)–Nb bridges in 1 and re-forming similar bridges intermolecularly. The effect of this process on the ^{1}H NMR spectra of 1 is unknown.

The crystal structure of 1 was refined previously in the monoclinic space group *Cc*.[26] We have redetermined the structure in the orthorhombic space group *F2dd*, which we believe to be correct. Details are given in the Experimental Section. The disorder among the bridging Cl, O, and OH ligands is still present in the new space group. Therefore, no comparison of distances or angles can be made. The average Nb–Cl(terminal) distance of 2.405 (6) Å is very similar to that observed in the two related compounds $[(\eta\text{-}C_5H_4SiMe_3)NbCl_2]_2(\mu\text{-}Cl)_2(\mu\text{-}O)$[6] and $[(\eta\text{-}C_5H_4SiMe_3)NbCl]_2(\mu\text{-}\eta^2\text{-}o\text{-}OC_6H_4O)_2(\mu\text{-}O)$.[7] Note however that the determination of this Nb–Cl distance will also suffer from the disorder in the crystals of 1, because of the different trans effects of the bridging ligands.

Reduction of 1 with Zinc Powder To Form $\{[(\eta\text{-}C_5Me_5)Nb(\mu\text{-}Cl)(\mu\text{-}O)]_3\}^+$ (2$^+$). When a solution of 1 in CH_2Cl_2 was stirred with zinc powder, the color of the solution changed to brown over a period of 10 min and then to green over 24 h. Removal of the excess zinc powder by filtration and layering of the CH_2Cl_2 solution with hexane or ether gave the cation **2**$^+$ (Figure 4) in combination with three different chlorozincate anions: $\{[ZnCl_2(\mu\text{-}Cl)]_2\}^{2-}$ (Figure 5), hereafter referred to as the $Zn_2Cl_6{}^{2-}$ salt; $\{[ZnCl]_4(\mu\text{-}Cl)_6\}^{2-}$ (Figure 6), the $Zn_4Cl_{10}{}^{2-}$ salt; $\{[ZnCl]_6(\mu\text{-}Cl)_8{}^{2-}\}_n$ (Figure 7), the $Zn_6Cl_{14}{}^{2-}$ salt. The structures of these chlorozincate anions are discussed below. In the case of the $Zn_4Cl_{10}{}^{2-}$ salt only, one of the two $\{[(\eta\text{-}C_5Me_5)Nb(\mu\text{-}Cl)(\mu\text{-}O)]_3\}^+$ cations for each anion had one of the bridging Cl ligands replaced by OH.[26] If this anomaly is set aside for the moment, the reduction of 1 to **2**$^+$ may be represented by eq 3.

$$3\ 1 + 2Zn \rightarrow 2\ 2^+ + 2Zn^{2+} + 3H^+ + 9Cl^- \quad (3)$$

We have not been able to completely define the conditions under which one or the other of chlorozincate anions is produced, although the nature of the nonsolvent added as precipitant plays some role (see Experimental Section). All the anions have the general formula $\{[Zn_xCl_{2x+2}]^{2-}\}_n$, and all contain tetrahedrally coordinated Zn^{2+}. It is probable that subtle changes in the concentration of **2**$^+$, the nature of the precipitating agent (ether or hexane), or temperature influenced which chlorozincate

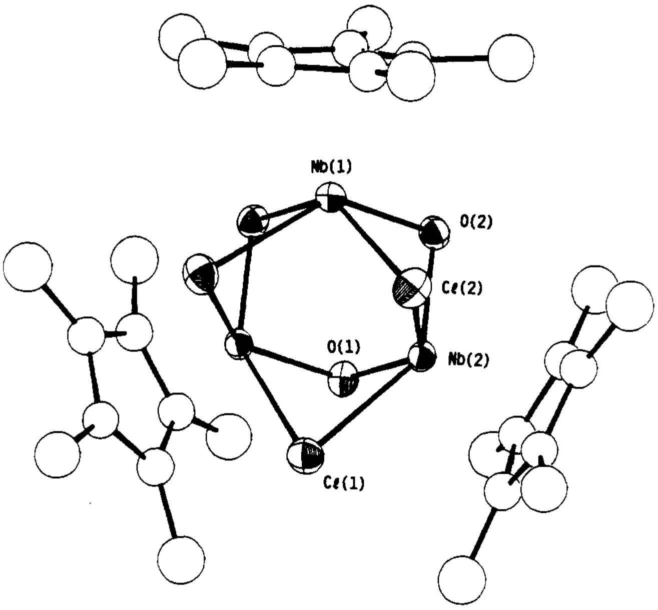

Figure 4. ORTEP plot of the structure of $\{[(\eta\text{-}C_5Me_5)Nb(\mu\text{-}Cl)(\mu\text{-}O)]_3\}^+$ (2^+).

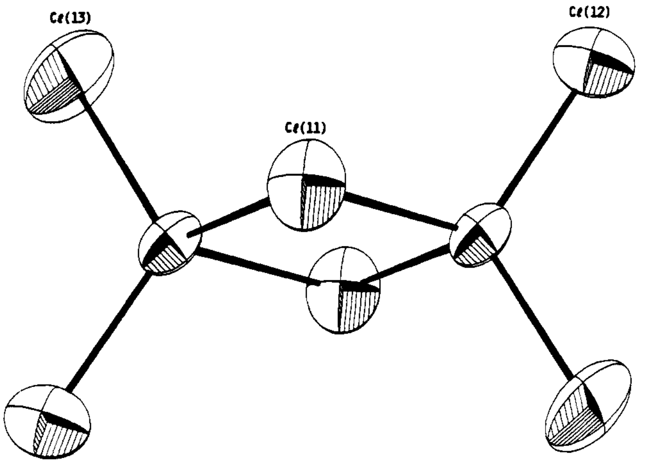

Figure 5. Structure of $\{[ZnCl_2(\mu\text{-}Cl)]_2\}^{2-}$.

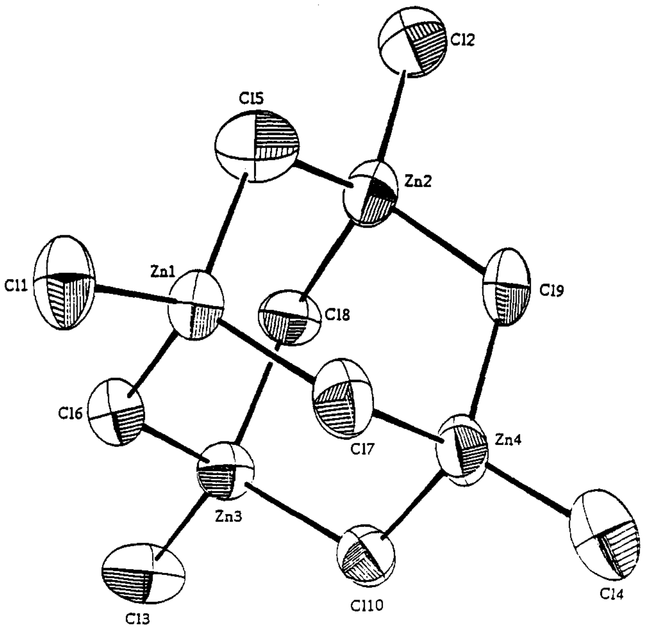

Figure 6. Structure of $\{[ZnCl]_4(\mu\text{-}Cl)_6\}^{2-}$.

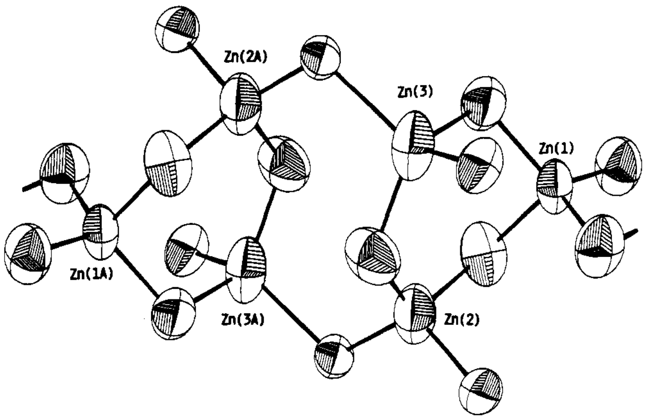

Figure 7. Structure of $\{[ZnCl]_6(\mu\text{-}Cl)_8\}^{2-}$.

anion was formed. It is noteworthy that crystals of 2^+ with any of the anions could only be obtained from CH_2Cl_2 solution. Reaction 3 appeared to proceed equally well in thf solution, but only $[Zn(thf)Cl(\mu\text{-}Cl)]_n$, which has previously been characterized by X-ray crystallography,[27] could be crystallized from such solutions. The Cl^- salt of 2^+, which was presumably present in solution after $[Zn(thf)Cl(\mu\text{-}Cl)]_n$ precipitated, was only obtained as an amorphous powder. The noncrystalline nature of 2^+Cl^- was probably due to the large difference in size between the anion and the cation. It appeared that the inability of CH_2Cl_2 to solvate $ZnCl_2$ led to the formation of the crystalline chlorozincate salts of 2^+.

The variability of the chlorozincate anion and the fact that the salts crystallized with different, and variable, amounts of solvent in the lattice (hexane in the case of the $Zn_2Cl_6^{2-}$ salt, $(C_2H_5)_2O$ and CH_2Cl_2 in the $Zn_4Cl_{10}^{2-}$ salt, no solvent of crystallization in the $Zn_6Cl_{14}^{2-}$ salt) made characterization of 2^+ by analytical methods very difficult and also made spectroscopic analysis very complicated. An additional complication was that the $Zn_4Cl_{10}^{2-}$ salt contained one 2^+ cation and one $\{[(\eta\text{-}C_5Me_5)Nb]_3(\mu\text{-}Cl)_2(\mu\text{-}OH)(\mu\text{-}O)_3\}^+$ cation for every $Zn_4Cl_{10}^{2-}$ anion. In $\{[(\eta\text{-}C_5Me_5)Nb]_3(\mu\text{-}Cl)_2(\mu\text{-}OH)(\mu\text{-}O)_3\}^+$ one of the μ-Cl ligands of 2^+ has been replaced by μ-OH.[26] This substitution does not markedly affect the electronic structure of the cation. The substitution of one OH for one Cl in 2^+ requires a source of oxygen (in addition to that provided by 1) in the reduction reaction 3. It is believed that this source was the zinc oxide coating on the zinc powder, since this coating has been found to act as a source of oxygen in reduction of other cyclopentadienyl–chloro–oxo complexes of niobium[8] and molybdenum.[2]

The reduction of orange 1 to green 2^+ proceeded via a brown intermediate. This intermediate was formed relatively rapidly from 1 and was converted more slowly to 2^+. It manifested a rather broad 10-line ESR signal, indicating a single unpaired electron on niobium, and it was much more sensitive to O_2 than diamagnetic 2^+. Efforts to characterize the brown intermediate are continuing.

As is discussed below, it was found that reduction of $\{[(\eta\text{-}C_5Me_5)NbCl]_3(\mu\text{-}Cl)(\mu\text{-}O)_2(\mu_3\text{-}OH)(\mu_3\text{-}O)\}^+$ (3^+, as the $Zn_2Cl_6^{2-}$ salt) with zinc also gave green 2^+. Compound 3^+ is closely related to the trinuclear compounds obtained by hydrolysis of $(\eta\text{-}C_5Me_5)NbCl_4$, and compound 1 is closely related to the dinuclear compounds produced by such hydrolysis.[19,24,25] Therefore it seems probably that reduction of any of these hydrolysis products with zinc will

---

[27] Bottomley, F.; Ferris, E. C.; White, P. S. *Acta Crystallogr.* **1989**, *45C*, 816.

Table I. Distances (Å) and Angles (deg) in $\{[(\eta\text{-C}_n\text{Me}_n)\text{M}(\mu\text{-A})_2]_3\}^{n+}$ Clusters

	$\{[(\eta\text{-C}_5\text{Me}_5)\text{Nb}(\mu\text{-Cl})(\mu\text{-O})]_3\}^+$	$\{[(\eta\text{-C}_6\text{Me}_6)\text{Nb}(\mu\text{-Cl})_2]_3\}^+$	$\{[(\eta\text{-C}_6\text{Me}_6)\text{Nb}(\mu\text{-Cl})_2]_3\}^{2+}$	$\{[(\eta\text{-C}_5\text{Me}_5)\text{Re}(\mu\text{-O})_2]_3\}^{2+}$
M–M	2.876 (1)	3.347 (2)	3.335 (9)	2.474 (2)
M–Cl	2.542 (1)	2.504 (2)	2.494 (3)	
M–O	1.937 (3)			1.96 (2)
M–Cp[a]	2.118 (5)			1.93 (3)
M–O–M	95.9 (1)			88.9 (1)
M–Cl–M	68.8 (3)	83.9 (1)	83.8 (1)	
Cl–M–Cl	79.2 (5)	83.1 (1)	83.4 (2)	
O–M–O	95.5 (1)			88.4 (1)
ref	this work	32	33	35

[a] Cp is the centroid of the C_5 ring of η-C_5Me_5; although the C_6Me_6 ring in $\{[(\eta\text{-C}_6\text{Me}_6)\text{Nb}(\mu\text{-Cl})_2]_3\}^{n+}$ is η^6, it is folded and there is no valid ring centroid.

Table II. Distances (Å) and Angles (deg) in the Three Salts of 2^+

	$Zn_2Cl_6^{2-}$	$Zn_4Cl_{10}^{2-}$	$Zn_6Cl_{14}^{2-}$
Nb–Nb	2.8753 (6)	2.863 (5)	2.855 (3)
Nb–Nb	2.8753 (6)	2.853 (5)	2.829 (3)
Nb–Nb	2.8769 (8)	2.861 (5)	2.825 (3)
Nb–Cl	2.537 (1), 2.537 (1)	2.537 (11), 2.561 (11)	2.494 (5), 2.428 (7)
Nb–Cl	2.548 (1), 2.542 (1)	2.521 (12), 2.559 (10)	2.495 (6), 2.435 (7)
Nb–Cl	2.548 (1), 2.542 (1)	2.524 (12), 2.525 (11)	2.465 (7), 2.476 (8)
Nb–O	1.943 (3), 1.943 (3)	1.98 (3), 1.93 (2)	1.894 (13), 1.922 (11)
Nb–O	1.935 (3), 1.932 (3)	1.91 (22), 1.92 (23)	1.925 (11), 1.895 (12)
Nb–O	1.935 (3), 1.932 (3)	1.96 (3), 1.929 (22)	1.941 (11), 1.922 (11)
Nb–Cp*	2.120 (5)	2.10 (4)	2.11 (4)
Nb–Cp*	2.120 (5)	2.10 (4)	2.13 (4)
Nb–Cp*	2.113 (5)	2.12 (4)	2.12 (5)
O–Nb–O	95.0 (1)	95.6 (10)	95.1 (5)
O–Nb–O	95.8 (1)	97.9 (10)	95.8 (5)
O–Nb–O	95.8 (1)	94.3 (11)	95.5 (5)
Cl–Nb–Cl	79.9 (4)	78.7 (3)	76.7 (2)
Cl–Nb–Cl	78.8 (5)	78.3 (4)	77.5 (2)
Cl–Nb–Cl	78.8 (5)	78.6 (4)	79.2 (2)
Nb–O–Nb	96.0 (2)	92.9 (11)	94.7_5 (5)
Nb–O–Nb	95.8 (1)	96.2 (10)	94.5_5 (5)
Nb–O–Nb	95.8 (1)	96.3 (10)	93.6 (5)
Nb–Cl–Nb	68.7 (4)	69.1 (3)	69.8 (2)
Nb–Cl–Nb	68.9 (3)	68.6 (3)	70.4 (2)
Nb–Cl–Nb	68.9 (3)	68.0 (3)	70.4 (2)
R	0.040	0.089	0.101

produce 2^+. However, the η-C_5Me_5 ligand is a necessity, since reduction of η-C_5H_5 derivatives did not give the analogue of 2^+.[8]

Physical Properties, Molecular Geometry, and Electronic Structure of 2^+. Cluster 2^+ was diamagnetic (as determined by both the Faraday and Evans methods[28]). It showed a single resonance at 2.10 ppm in the ^1H NMR spectrum, assigned to the protons of the η-$C_5(CH_3)_5$ ligand. However, this signal was flanked by a number of very much weaker resonances at 2.07, 2.06, and 2.04 ppm. Likewise, the ^{13}C NMR spectrum showed an intense resonance at 127.8 ppm (assigned to $C_5(CH_3)_5$) and satellites at 126.7 and 126.5 ppm, as well as an intense resonance at 11.8 ppm with satellites at 11.5 and 11.4 ppm (assigned to $C_5(CH_3)_5$). The relative intensities of these signals varied from preparation to preparation but did not vary with time or temperature within a single preparation. Two reasons may be advanced for the observation of these satellite resonances. The first is that some of the μ-Cl atoms in 2^+ may be replaced by μ-OH, as described above. This is unlikely to take place on a large scale because of the low concentration of OH^-. The second is that 2^+ may exhibit isomerism. In all of the salts of 2^+ which were examined by X-ray difrraction, the oxygen atoms lie on one side of the Nb_3 plane, with the chlorine atoms on the other. However, the location of one oxygen and one chlorine could be interchanged. Interconversion could only occur by disruption of the $[\text{Nb}(\mu\text{-Cl})(\mu\text{-O})]_3$ ring, but the formation of isomers during the reduction of 1 to 2^+ may occur.

The structure of 2^+ is shown in Figure 4, and the important bond distances and angles are collected in Table I. The parameters for 2^+ in this table are taken from the structural determination of the $Zn_2Cl_6^{2-}$ salt, for the reasons discussed below. A detailed listing of distances and angles for all the salts is given in Table II. From Figure 4 and Table I, it is seen that 2^+ contains an equilateral triangle of niobium atoms, the edges of which are bridged by oxygen and chlorine atoms. All the chlorine atoms are on one side of the Nb_3 plane, and all the oxygen atoms on the other. The crystallographically imposed symmetry of the $Zn_2Cl_6^{2-}$ salt of 2^+ is C_{2v}, but the effective symmetry is C_{3v}.

Table I also compares the distances and angles in 2^+ with those in $\{[(\eta\text{-C}_6\text{Me}_6)\text{Nb}(\mu\text{-Cl})_2]_3\}^{n+}$ (n = 1,[29–31] 2[32]) and in $\{[(\eta\text{-C}_5\text{Me}_5)\text{Re}(\mu\text{-O})]_3\}^{2+}$.[33–35] It is immediately clear that there are no significant differences in any distances or angles between the two $\{[(\eta\text{-C}_6\text{Me}_6)\text{Nb}(\mu\text{-Cl})_2]_3\}^{n+}$ cations. It is also clear that the average Nb–Nb distance in 2^+ is very much shorter (by 0.46 Å) than that in $\{[(\eta\text{-C}_6\text{Me}_6)\text{Nb}(\mu\text{-Cl})_2]_3\}^{n+}$. The average Nb–Nb distance in 2^+ (2.876 (1) Å) is, however, very similar to the average Re–Re distance in $\{[(\eta\text{-C}_5\text{Me}_5)\text{Re}(\mu\text{-O})_2]_3\}^{2+}$ (2.747 (2) Å) when the smaller covalent radius of Re[36] is taken into account. A third difference, although of less statistical significance (see below), is that the average Nb–Cl distance in 2^+ is 0.04 Å longer than that in $\{[(\eta\text{-C}_6\text{Me}_6)\text{Nb}(\mu\text{-Cl})_2]_3\}^{n+}$. Since 2^+ formally contains Nb_3^{13+} and $\{[(\eta\text{-C}_6\text{Me}_6)\text{Nb}(\mu\text{-Cl})_2]_3\}^{n+}$ contain Nb_3^{7+} for $n = 1$ and Nb_3^{8+} for $n = 2$, it would be expected that the average Nb–Cl distance in 2^+ would be considerably shorter than in the $\{[(\eta\text{-C}_6\text{Me}_6)\text{Nb}(\mu\text{-Cl})_2]_3\}^{n+}$ cations, contrary to what is observed. The fourth difference is that the average Nb–O distance in 2^+ is 1.937 (3) Å, which is 0.02 Å shorter than the average Re–O distance in $\{[(\eta\text{-C}_5\text{Me}_5)\text{Re}(\mu\text{-O})_2]_3\}^{2+}$. The smaller size of Re, coupled with the higher formal charge on Re (Re_3^{17+} versus Nb_3^{13+})

---

(28) Evans, D. F.; Fazakerley, G. V.; Phillips, R. F. *J. Chem. Soc. A* 1971, 1931.

(29) Fischer, E. O.; Röhrscheid, F. *J. Organomet. Chem.* **1966**, *6*, 53.

(30) Churchill, M. R.; Chang, S. W.-Y. *J. Chem. Soc.* **1974**, 248.

(31) Stollmaier, F.; Thewalt, U. *J. Organomet. Chem.* **1981**, *222*, 227.

(32) Goldberg, S. Z.; Spivack, B.; Stanley, G.; Eisenberg, R.; Braitsch, D. M.; Miller, J. S.; Abkowitz, M. *J. Am. Chem. Soc.* **1977**, *99*, 110.

(33) Herrmann, W. A.; Serrano, R.; Ziegler, M. L.; Pfisterer, H.; Nuber, B. *Angew. Chem., Int. Ed. Engl.* **1985**, *24*, 50.

(34) Herrmann, W. A.; Serrano, R.; Küsthardt, U.; Guggolz, E.; Nuber, B.; Ziegler, M. L. *J. Organomet. Chem.* **1985**, *287*, 329.

(35) Hofmann, P.; Rösch, N.; Schmidt, H. R. *Inorg. Chem.* **1986**, *25*, 4470.

(36) Butler, I. S.; Harrod, J. F. *Inorganic Chemistry*; Benjamin/Cummings: Don Mills, Ontario, Canada, 1989; p 48.

should lead to an Nb–O distance considerably longer than Re–O. Note that a simple averaging of the Nb–O distances in all the salts of 2^+ (see Table II) gives a distance of 1.930 (13) Å. Simple averaging of all the Nb–Cl distances gives 2.515 (6) Å. Therefore, the discussion of the Nb–O and Nb–Cl distances is unaffected by statistical considerations. The observation that the M–C distances to the η-C_5Me_5 or η-C_6Me_6 rings follow the trends expected on the basis of the charge and covalent radius of M further indicates that the observed trends in the M–O and M–Cl distances are significant.

The number of cluster electrons is two in 2^+ (Nb_3^{13+}), eight in $\{[(\eta\text{-}C_6Me_6)Nb(\mu\text{-}Cl)_2]_3\}^+$ (Nb_3^{7+}), seven in $\{[(\eta\text{-}C_6Me_6)Nb(\mu\text{-}Cl)_2]_3\}^{2+}$ (Nb_3^{8+}), and four in $\{[(\eta\text{-}C_5Me_5)Re(\mu\text{-}O)_2]_3\}^{2+}$ (Re_3^{17+}). The energy level ordering of the cluster orbitals of $\{[(\eta\text{-}C_5Me_5)Re(\mu\text{-}O)_2]_3\}^{2+}$ and $\{[(\eta\text{-}C_6Me_6)Nb(\mu\text{-}Cl)_2]_3\}^{n+}$ was analyzed, using both extended Hückel and SCF Xα–SW methods, by Hofmann, Rösch, and Schmidt.[35] The fact that 2^+ is diamagnetic confirms the level ordering of $1a_1' < 1e' < 2a_1' < 2e'$ proposed by them, since the two cluster electrons of 2^+ will occupy the $1a_1'$ level. The calculations of Hofmann, Rösch, and Schmidt suggested that there was little direct metal–metal bonding in any of the $\{[(\eta\text{-}C_5Me_5)Re(\mu\text{-}O)_2]_3\}^{2+}$ or $\{[(\eta\text{-}C_6Me_6)Nb(\mu\text{-}Cl)_2]_3\}^{n+}$ ions. The large differences in the M–M distances were due to the strong Re–O bonding, particularly π bonding, compared to the Nb–Cl bonding. This would be reinforced by the high formal charge on rhenium (Re_3^{17+}) compared to niobium (Nb_3^{7+}, Nb_3^{8+}). The percentage of oxygen character in the cluster orbitals was estimated (by the extended Hückel method) to be 30 for $1a_1'$, 29 for $1e'$, 49 for $2a_1'$, and 24 for $2e'$ in $\{[(\eta\text{-}C_5Me_5)Re(\mu\text{-}O)_2]_3\}^{2+}$. The chlorine contribution to the cluster orbitals of $\{[(\eta\text{-}C_6Me_6)Nb(\mu\text{-}Cl)_2]_3\}^{n+}$ was not given, but the calculated niobium contribution to these orbitals (in percent) was 92 for $1a_1'$, 75 for $1e'$, 63 for $2a_1'$, and 87 for $2e'$. Therefore the chlorine contribution must be much smaller than that of oxygen.

It is clear from the distances given above that 2^+ does not behave as a mixture of $\{[(\eta\text{-}C_5Me_5)Re(\mu\text{-}O)_2]\}_3^{2+}$ and $\{[(\eta\text{-}C_6Me_6)Nb(\mu\text{-}Cl)_2]_3\}^{n+}$ but closely resembles $\{[(\eta\text{-}C_5Me_5)Re(\mu\text{-}O)_2]_3\}^{2+}$. However, the Nb–O distance in 2^+ is even shorter than the Re–O distance in $\{[(\eta\text{-}C_5Me_5)Re(\mu\text{-}O)_2]_3\}^{2+}$. One reason for this is that in $\{[(\eta\text{-}C_5Me_5)Re(\mu\text{-}O)_2]_3\}^{2+}$ the metal orbitals available for M–O π bonding must be shared by four oxygen atoms per metal, but in 2^+ they are shared by only two oxygen atoms per metal. A second reason is that the cluster orbitals represent the M–O π-antibonding interaction. To the extent that these orbitals are occupied, the M–O bonds will be weakened. Each of the cluster orbitals which are occupied in 2^+ or in $\{[(\eta\text{-}C_5Me_5)Re(\mu\text{-}O)_2]_3\}^{2+}$ has approximately the same oxygen contribution. In $\{[(\eta\text{-}C_5Me_5)Re(\mu\text{-}O)_2]_3\}^{2+}$ the cluster orbitals are occupied by four electrons ($1a_1'^2\ 1e'^2$). In 2^+ only the $1a_1'$ orbital is occupied, and the M–O π bonding will be correspondingly stronger.

The above arguments explain quite well why the Nb–Nb distances in 2^+ are similar to those in $\{[(\eta\text{-}C_5Me_5)Re(\mu\text{-}O)_2]_3\}^{2+}$ but much shorter than those in $\{[(\eta\text{-}C_6Me_6)Nb(\mu\text{-}Cl)_2]_3\}^{n+}$. It is much less clear why the Nb–Cl distances in 2^+ are longer than those in $\{[(\eta\text{-}C_6Me_6)Nb(\mu\text{-}Cl)_2]_3\}^{n+}$. There is no obvious electronic reason. It has been noted previously that a strongly π-bonded oxygen has a large trans effect.[37-39] The oxygen and chlorine atoms in 2^+ may be regarded as being approximately trans to one another, but the calculations by Hofmann, Rösch, and Schmidt[35] suggested that there would be little contribution by chlorine to the shared orbitals on niobium. It is also possible that the chlorine atoms in 2^+ are forced away from the metal by repulsion due to the electrons in the multiply bonded Nb–O unit. Finally, as noted below, the apparent lengthening of the Nb–Cl distances in 2^+ compared to those in $\{[(\eta\text{-}C_6Me_6)Nb(\mu\text{-}Cl)_2]_3\}^{n+}$ may not be real because the spread in the Nb–Cl distances is large when the salts of 2^+ with different chlorozincate anions are compared. In $[(\eta\text{-}C_5H_5)NbCl(\mu\text{-}Cl)]_3(\mu_3\text{-}OH)(\mu_3\text{-}O)$ the Nb–Cl distances to the bridging chlorine atoms average 2.532 (1) Å, with a range of 0.06 Å.[8]

One of the problems with $\{[(\eta\text{-}C_5Me_5)Re(\mu\text{-}O)_2]_3\}^{2+}$ which was addressed by Hofmann, Rösch, and Schmidt[35] was the lack of transfer of spin density from the unpaired electrons in the cluster core to the protons of the η-$C_5(CH_3)_5$ ligand. This lack of transfer of spin density occurred also in $[(\eta\text{-}C_5Me_5)V]_4(\mu\text{-}O)_6$, which was a simple paramagnetic species with $\mu_{eff} = 2.90\ \mu_B$ (by the Faraday method at 295 K). The magnetic moment was in agreement with extended Hückel calculations, which indicated an $a_1^2\ e^2$ ground state.[40] This is rather similar to $\{[(\eta\text{-}C_5Me_5)Re(\mu\text{-}O)_2]_3\}^{2+}$, and like that cluster, $[(\eta\text{-}C_5Me_5)V]_4(\mu\text{-}O)_6$ showed a single sharp resonance in the ^1H NMR spectrum at 2.00 ppm, i.e. in the diamagnetic region. The antiferromagnetic cubane $[(\eta\text{-}C_5Me_5)Cr(\mu_3\text{-}O)]_4$, with 12 cluster electrons, showed a moderately broadened resonance at −2.46 ppm (in $CDCl_3$ solution).[1] This is shifted from the normal region for resonances of η-$C_5(CH_3)_5$ in diamagnetic complexes, although not by a large amount. On the other hand, the ^1H resonance of η-C_5H_5 in $[(\eta\text{-}C_5H_5)Cr(\mu_3\text{-}O)]_4$ was found at −31.6 ppm (at 298 K) and was extremely broad.[41] The lack of transfer of spin density in the η-C_5Me_5 derivatives appears to be due less to the low contribution of η-C_5R_5 orbitals to the cluster orbitals than to the difficulty of transfer through the σ bonds of the $C\text{–}CH_3$ moiety.

The marked green color of 2^+ is due to an absorption band at 580 nm, which has an extinction coefficient of 100. The Xα–SW calculations of Hofmann, Rösch, and Schmidt on $\{[(\eta\text{-}C_5Me_5)Re(\mu\text{-}O)_2]_3\}^{2+}$ indicated that the energy difference between the $1a_1'$ and $1e'$ cluster orbitals was approximately 1 eV.[35] However, this gap was filled with orbitals which were derived from the η-C_5R_5 π-molecular orbitals. The low energy of the absorption band at 580 nm in 2^+ suggests that it is due to a transition from a η-C_5Me_5 π orbital to $1e'$, which is a ligand-to-metal charge-transfer band. However, the low intensity is not in agreement with such a transition. In $\{[(\eta\text{-}C_6Me_6)Nb(\mu\text{-}Cl)_2]_3\}^+$ the η-C_6Me_6 π orbitals lie at much lower energies,[35] and the electronic transitions lie at higher energies (420 nm[42]) than in 2^+. However, they are also much more intense ($\epsilon \simeq 40\,000$[42]). Although the increase in energy is in agreement with the transitions being localized in the cluster orbitals, the very high intensity is indicative of a charge-transfer band.

Chemical Properties of 2^+. In the solid state 2^+ was decomposed only very slowly by air. In CH_2Cl_2 solution oxidation by O_2 gave $\{[(\eta\text{-}C_5Me_5)NbCl]_3(\mu\text{-}Cl)(\mu\text{-}O)_2(\mu_3\text{-}OH)(\mu_3\text{-}O)\}^+$ (3^+) (see Figure 8), isolated as the $Zn_2Cl_6^{2-}$ salt. The oxidation of 2^+ to 3^+ was independent of the nature

---

[37] Herrmann, W. A.; Küsthardt, U.; Flöel, M.; Kulpe, J.; Herdtweck, E.; Voss, E. *J. Organomet. Chem.* **1986**, *314*, 151.

[38] Herrmann, W. A.; Herdtweck, E.; Flöel, M.; Kulpe, J.; Küsthardt, U.; Okuda, J. *Polyhedron* **1987**, *6*, 1165.

[39] Herrmann, W. A.; Jung, K. A.; Herdtweck, E. *Chem. Ber.* **1989**, *122*, 2041.

[40] Bottomley, F.; Magill, C. P.; Zhao, B. *Organometallics*, **1991**, *10*, 1946.

[41] Bottomley, F.; Paez, D. E.; Sutin, L.; White, P. S.; Köhler, F. H.; Thompson, R. C.; Westwood, N. P. C. *Organometallics* **1990**, *9*, 2443.

[42] King, R. B.; Braitsch, D. M.; Kapoor, P. N. *J. Am. Chem. Soc.* **1975**, *97*, 60.

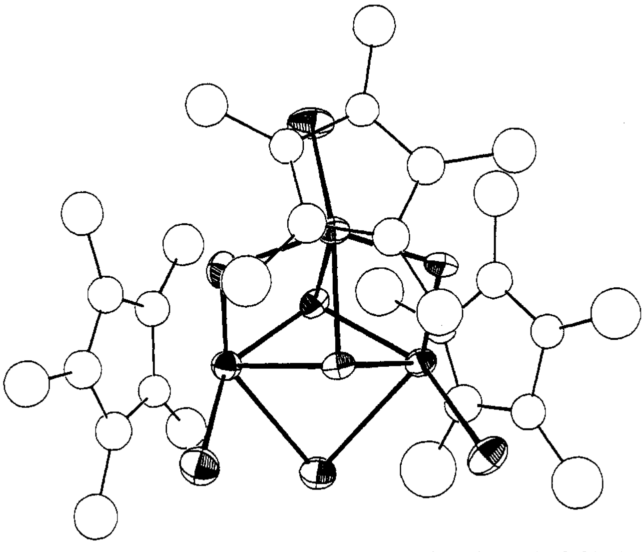

Figure 8. ORTEP plot of the structure of $\{[(\eta\text{-}C_5Me_5)NbCl]_3(\mu\text{-}Cl)(\mu\text{-}O)_2(\mu_3\text{-}OH)(\mu_3\text{-}O)\}^+$ (3^+).

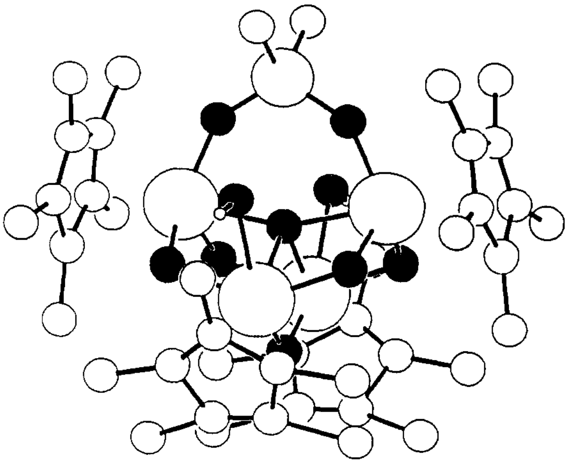

Figure 9. Structure of $[(\eta\text{-}C_5Me_5)Nb]_4(OH)_2(\mu\text{-}O)_5(\mu_4\text{-}O)(\mu\text{-}O_2SiMe_2)$.

of the chlorozincate anion. Inspection of the formulas of 2^+ and 3^+ reveals that the oxidation adds one O, one Cl, and one H atom to 2^+. The yield of 3^+ was 70%, based on niobium and after recrystallization. No product containing niobium, other than 3^+, could be identified. Therefore the Cl and H atoms must come from the CH_2Cl_2 solvent, and the oxidation can be formally represented by eq 4.

$$2\{[(\eta\text{-}C_5Me_5)Nb(\mu\text{-}Cl)(\mu\text{-}O)]_3\}_2Zn_2Cl_6 + 2O_2 + CH_2Cl_2 \rightarrow 2\{[(\eta\text{-}C_5Me_5)NbCl]_3(\mu\text{-}Cl)(\mu\text{-}O)_2(\mu_3\text{-}OH)(\mu_3\text{-}O)\}_2Zn_2Cl_6 + CO_2 \quad (4)$$

The redox reaction (4) is clearly a complicated process which involves cleavage of C–H and C–Cl bonds of the solvent. During attempts to define the role of the solvent in the oxidation of 2^+ to 3^+, we isolated the cluster $[(\eta\text{-}C_5Me_5)Nb]_4(OH)_2(\mu\text{-}O)_5(\mu_4\text{-}O)(\mu\text{-}O_2SiMe_2)$ (Figure 9). This was identified by a partial structural analysis. In this compound the Si–C bonds of the silicone grease used on joints and stopcocks has been cleaved. The cluster $[(\eta\text{-}C_5Me_5)Nb]_4(OH)_2(\mu\text{-}O)_5(\mu_4\text{-}O)(\mu\text{-}O_2SiMe_2)$ is closely related to $[(\eta\text{-}C_5Me_5)Ta]_4(OH)_2(\mu\text{-}O)_4(\mu_3\text{-}O)_2(\mu_4\text{-}O)$, isolated by Gibson and Kee.[22] It is not clear why oxidation of these niobium(IV) compounds by O_2 proceeds only with concomitant C–H, C–Cl, or C–Si bond cleavage.

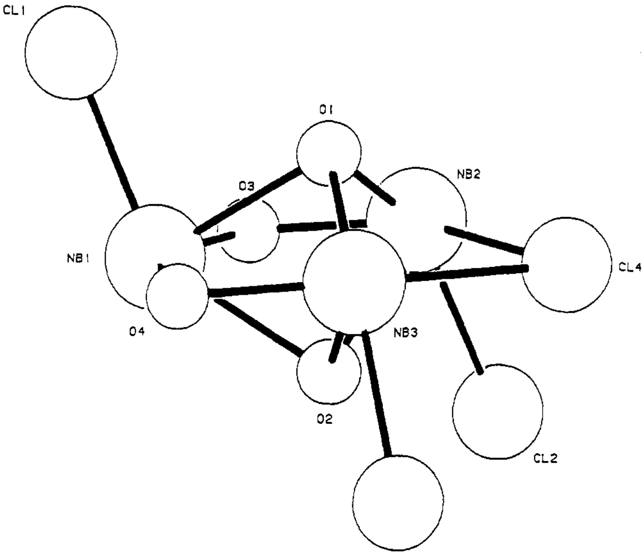

Figure 10. The $[NbCl]_3(\mu\text{-}Cl)(\mu\text{-}O)_2(\mu_3\text{-}OH)(\mu_3\text{-}O)$ core of 3^+.

Table III. Important Distances (Å) and Angles (deg) in 3^{+a}

Nb(1)–Nb(2)	3.018 (2)	Nb(3)–O(2)	2.185 (8)
Nb(1)–Nb(3)	3.038 (2)	Nb(2)–Cl(4)	2.628 (4)
Nb(2)–Nb(3)	3.318 (2)	Nb(3)–Cl(4)	2.588 (4)
Nb(1)–Cl(1)	2.338 (4)	Nb(1)–O(3)	1.973 (8)
Nb(2)–Cl(2)	2.399 (4)	Nb(1)–O(4)	1.956 (8)
Nb(3)–Cl(3)	2.398 (4)	Nb(2)–O(3)	1.895 (9)
Nb(1)–O(1)	2.228 (8)	Nb(3)–O(4)	1.914 (8)
Nb(1)–O(2)	2.234 (8)	Nb(1)–Cp(1)[b]	2.14 (1)
Nb(2)–O(1)	2.027 (8)	Nb(2)–Cp(2)	2.14 (1)
Nb(2)–O(2)	2.203 (8)	Nb(3)–Cp(3)	2.15 (1)
Nb(3)–O(1)	2.065 (8)		

Nb(1)–O(1)–Nb(2)	90.2 (3)	O(1)–Nb(3)–O(2)	66.0 (3)
Nb(1)–O(1)–Nb(3)	90.0 (3)	Nb(2)–Cl(4)–Nb(3)	79.0 (1)
Nb(2)–O(1)–Nb(3)	108.4 (4)	Nb(1)–O(3)–Nb(2)	102.6 (4)
Nb(1)–O(2)–Nb(2)	85.7 (3)	Nb(1)–O(4)–Nb(3)	103.4 (4)
Nb(1)–O(2)–Nb(3)	86.9 (3)	O(3)–Nb(1)–O(4)	141.6 (3)
Nb(2)–O(2)–Nb(3)	98.3 (3)	O(3)–Nb(2)–Cl(4)	145.7 (3)
O(1)–Nb(1)–O(2)	62.5 (3)	O(4)–Nb(3)–Cl(4)	145.6 (3)
O(1)–Nb(2)–O(2)	66.2 (3)		

[a] For the numbering scheme, see Figure 10. [b] Cp is the centroid of the C_5 ring.

Structure of $\{[(\eta\text{-}C_5Me_5)NbCl]_3(\mu\text{-}Cl)(\mu\text{-}O)_2(\mu_3\text{-}OH)(\mu_3\text{-}O)\}^+$ (3^+). An ORTEP[43] diagram of 3^+ is given in Figure 8, and the core (with atom numbering) is shown in Figure 10. Important distances and angles are given in Table III. The structure of 3^+ is rather similar to those of the M(V) (M = Nb, Ta) trinuclear clusters $[(\eta\text{-}C_5Me_5)MCl]_3(\mu\text{-}Cl)(\mu\text{-}O)_3(\mu_3\text{-}O)$ (M = Nb,[23,25] Ta[19,24]), $\{[(\eta\text{-}C_5Me_5)_3Ta_3Cl(H_2O)_2](\mu\text{-}O)_3(\mu_3\text{-}O)_2\}^+$,[24] and $\{[(\eta\text{-}C_5Me_5)_3Nb_3Cl(OH)_2](\mu\text{-}OH)(\mu\text{-}O)_2(\mu_3\text{-}OH)(\mu_3\text{-}O)\}^+$[25] and to $[(\eta\text{-}C_5Me_5)ZrCl]_3(\mu\text{-}OH)_3(\mu_3\text{-}OH)(\mu_3\text{-}O)$.[44] The core of cluster 3^+ also resembles those in $[\{(\eta\text{-}C_5H_5)NbCl(\mu\text{-}Cl)\}_3(\mu_3\text{-}OH)(\mu_3\text{-}O)]$[3,8] and $[Mo(OR)_2(\mu\text{-}OR)]_3(\mu_3\text{-}OR)(\mu_3\text{-}O)$ (R = $CH(CH_3)_2$).[45] Because of the uncertainty in locating the hydrogen atoms in these compounds, it is quite possible that $\{[(\eta\text{-}C_5Me_5)_3Ta_3Cl(H_2O)_2](\mu\text{-}O)_3(\mu_3\text{-}O)_2\}^+$[24] and $\{[(\eta\text{-}C_5Me_5)_3Nb_3Cl(OH)_2](\mu\text{-}OH)(\mu\text{-}O)_2(\mu_3\text{-}OH)(\mu_3\text{-}O)\}^+$[25] have the same structure or that the true structures are not

---

(43) Johnson, C. K. *ORTEP-II: A FORTRAN Thermal Ellipsoid Plot Program for Crystal Structure Illustrations*; Report ORNL-5138; Oak Ridge National Laboratory: Oak Ridge, TN, 1976.

(44) Babcock, L. M.; Day, V. W.; Klemperer, W. G. *J. Chem. Soc., Chem. Commun.* **1988**, 519.

(45) Chisholm, M. H.; Folting, K.; Huffman, J. C.; Kirkpatrick, C. C. *J. Am. Chem. Soc.* **1981**, *103*, 5967.

represented by either of these formulas. This problem was also encountered in the determination of the structure of 3^+. No unequivocal evidence for an OH hydrogen was found in a final difference Fourier synthesis. The position of the hydrogen atom, and therefore the structural formula of 3^+, was decided on the basis of the Nb–O distances and the effective symmetry of the cation. The μ-O atoms O(3) and O(4) (Figure 10) have equivalent bonding environments between Nb(1) and Nb(2) or Nb(3), respectively. Only disorder, for which there was no evidence, could accommodate one of these atoms as OH. The μ_3-O(1) atom is very asymmetrically bonded to the three Nb atoms (see below). However, the Nb–μ_3-O(2) distances are all longer than Nb–O(1). Therefore, O(2) was assigned as the OH group.

Cluster 3^+ has an isosceles triangle of Nb atoms (Nb(1)–Nb(2) = 3.018 (2) Å, Nb(1)–Nb(3) = 3.038 (2) Å, Nb(2)–Nb(3) = 3.318 (2) Å), the long edge of which is bridged by Cl. Such an isosceles triangle was also observed in the M(V) clusters $[(\eta\text{-}C_5Me_5)MCl]_3(\mu\text{-}Cl)(\mu\text{-}O)_3(\mu_3\text{-}O)$ (M = Nb,[23,25] Ta[19,24]), $\{[(\eta\text{-}C_5Me_5)_3Ta_3Cl(H_2O)_2](\mu\text{-}O)_3(\mu_3\text{-}O)_2\}^+$,[24] and $\{[(\eta\text{-}C_5Me_5)_3Nb_3Cl(OH)_2](\mu\text{-}OH)(\mu\text{-}O)_2(\mu_3\text{-}OH)(\mu_3\text{-}O)\}^+$.[25] In the Nb(IV) cluster $[(\eta\text{-}C_5H_5)NbCl(\mu\text{-}Cl)]_3(\mu_3\text{-}OH)(\mu_3\text{-}O)$ there is also an isosceles triangle, but in this case one Nb–Nb distance is much shorter than the other two,[3,8] not longer as in 3^+. The clusters $[(\eta\text{-}C_5Me_5)ZrCl]_3(\mu\text{-}OH)_3(\mu_3\text{-}OH)(\mu_3\text{-}O)$ and $[Mo(OR)_2(\mu\text{-}OR)]_3(\mu_3\text{-}OR)(\mu_3\text{-}O)$ have equilateral triangles of metal atoms. The major difference between 3^+ and the related compounds is that the μ_3-O atom in 3^+ is neither symmetrically bridged, as it is in the clusters with equilateral triangles of metal atoms and also in $[(\eta\text{-}C_5H_5)NbCl(\mu\text{-}Cl)]_3(\mu_3\text{-}OH)(\mu_3\text{-}O)$[3,8] and $\{[(\eta\text{-}C_5Me_5)_3Nb_3Cl(OH)_2]_2(\mu\text{-}OH)](\mu\text{-}O)_2(\mu_3\text{-}OH)(\mu_3\text{-}O)\}^+$ (which have isosceles triangles), nor is it so unsymmetrically bridged that it is μ_2-O rather than μ_3-O. In those compounds with a μ_2-O, the Nb–O bonding distances average 1.99 Å and the distance to the third niobium averages 2.67 Å, whereas in 3^+ the Nb–O(1) distances are Nb(1)–O(1) = 2.228 (8) Å, Nb(2)–O(1) = 2.027 (8) Å, and Nb(3)–O(1) = 2.065 (8) Å. The Nb–O(2) distances (these involving the OH group) are much more symmetrical at 2.234 (8), 2.203 (8), and 2.185 (8) Å, respectively. The asymmetry in 3^+ is also manifested in the Nb–Cl distances (Nb(1)–Cl(1) = 2.388 (4) Å, Nb(2)–Cl(2) = 2.399 (4) Å, Nb(3)–Cl(3) = 2.398 (4) Å). However, the Nb–(μ_2-O) distances have the opposite trend: those to Nb(1) are longer (1.973 (8) and 1.956 (8) Å) than to Nb(2) and Nb(3) (1.895 (9) and 1.914 (8) Å). The Nb–Cp distances are constant (Nb(1)–Cp(1) = 2.14 (1) Å, Nb(2)–Cp(2) = 2.14 (1) Å, Nb(3)–Cp(3) = 2.15 (1) Å). These contradictory trends indicate that the coordination number of the niobium atoms does not play a large role in the geometrical details of 3^+ and related clusters. There must be a very delicate balance in energy between seven or eight coordination of niobium and two or three coordination of oxygen in these compounds.

The propensity of (cyclopentadienyl)niobium chloride oxides and -tantalum chloride oxides to form triangular clusters is as noticeable as it is inexplicable. The oxidation state of niobium is not a factor, since 3^+ and its relatives contain Nb_3^{15+}, $[(\eta\text{-}C_5H_5)NbCl(\mu\text{-}Cl)]_3(\mu_3\text{-}OH)(\mu_3\text{-}O)$ contains Nb_3^{12+}, and 2^+ contains Nb_3^{13+}. The only clusters with more than three niobium or tantalum atoms are the four-metal butterfly clusters $[(\eta\text{-}C_5Me_5)Nb]_4(OH)_2(\mu\text{-}O)_5(\mu_4\text{-}O)(\mu\text{-}O_2SiMe_2)$ (Figure 9) and $[(\eta\text{-}C_5Me_5)Ta]_4(OH)_2(\mu\text{-}O)_4(\mu_3\text{-}O)_2(\mu_4\text{-}O)$[22] and the ill-defined cluster $(\eta\text{-}C_5H_4Me)_4Nb_5Cl_5(OH)_9O(thf)_2$, which contains a tetrahedron of niobium atoms.[8] All other clusters are trinuclear.

Table IV. Distances (Å) and Angles (deg) in the $Zn_2Cl_6^{2-}$ and $Zn_4Cl_{10}^{2-}$ Anions

	$Zn_2Cl_6^{2-}$ (2^+)	$Zn_2Cl_6^{2-}$ (3^+)	$Zn_4Cl_{10}^{2-}$
Zn–Cl(term)	2.197 (3)	2.188 (6)	2.181 (12)
Zn–Cl(bridg)	2.355 (2)	2.359 (5)	2.297 (12)
Cl(term)–Zn–Cl(term)	115.5 (1)	116.3 (3)	
Cl(term)–Zn–Cl(bridg)	111.4 (6)	111.3 (2)	111.4 (4)
Cl(bridg)–Zn–Cl(bridg)	93.5 (1)	92.3 (2)	107.4 (5)
Zn–Cl–Zn	86.5 (1)	87.7 (2)	113.3 (4)

The Chlorozincate Anions. Three different chlorozincate anions were observed in the present investigations: $\{[ZnCl_2(\mu\text{-}Cl)]_2\}^{2-}$ (Figure 5), found as the anion to 2^+ and to 3^+; $\{[ZnCl]_4(\mu\text{-}Cl)_6\}^{2-}$ (Figure 6) and $(\{[ZnCl]_6(\mu\text{-}Cl)_8\}^{2-})_n$ (Figure 7), both found as the anion to 2^+. All the anions have tetrahedrally coordinated zinc. The first has been observed previously by Cotton and co-workers[46] as the anion to $\{[V(thf)_3]_2(\mu\text{-}Cl)_3\}^+$,[47] and the structure observed here is essentially identical. The adamantane-like $\{[ZnCl]_4(\mu\text{-}Cl)_6\}^{2-}$ appears to fill a gap in the known compounds of group 12 having the adamantane-like core. Whereas compounds of general formula $\{[Zn(SR)]_4(\mu\text{-}SR)_6\}^{2-}$ and $\{[ZnCl]_4(\mu\text{-}SR)_6\}^{2-}$ have been extensively studied,[47-49] the simple halide $\{[ZnCl]_4(\mu\text{-}Cl)_6\}^{2-}$ has not been observed previously. The chain-of-rings structure of $(\{[ZnCl]_6(\mu\text{-}Cl)_8\}^{2-})_n$ (Figure 7) also appears to be novel. In this case serious disorder prevents a detailed discussion of the structure. The average distances and angles in $\{[ZnCl_2(\mu\text{-}Cl)]_2\}^{2-}$ and $\{[ZnCl]_4(\mu\text{-}Cl)_6\}^{2-}$ are given in Table IV.

A Note on Estimated Standard Deviations and the Structure of 2^+. In the present work the structure of 2^+ was determined three times, with three different anions. Although there was disorder in the anions, and in the solvents of crystallization (where present), and although in one case a cocation $(\{[(\eta\text{-}C_5Me_5)Nb]_3(\mu\text{-}Cl)_2(\mu\text{-}OH)(\mu\text{-}O)_3\}^+)$ was present, there was no evidence of disorder in the $[Nb(\mu\text{-}Cl)(\mu\text{-}O)]_3$ core of the cation 2^+. The determination of the structure of $\{2^+\}_2\{Zn_2Cl_6^{2-}\}$ was considered to be very accurate, and the parameters of this salt were used in the discussion above. The determination of the structure of $\{2^+\}_2\{Zn_4Cl_{10}^{2-}\}$ was deemed to be less accurate but was certainly acceptable, particularly if the criteria of the esd's in the bond distances is used as the criterion of acceptability (see Table II). The structure determined for $\{2^+\}_2\{Zn_6Cl_{14}^{2-}\}$ was much less reliable, although the esd's in Table II suggest that the structure is more accurate than that of $\{2^+\}_2\{Zn_4Cl_{10}^{2-}\}$. When the data in Table II are examined, it appears that there are major differences between $[Nb(\mu\text{-}Cl)(\mu\text{-}O)]_3$ cores in the three salts. For example, the spread in the Nb–Cl distances is 0.11 Å and the maximum esd of these distances is 0.012. However, the esd's assume only random errors in the data and do not take into account the systematic errors introduced, for example, by the inadequate treatment of disorder. Due caution must be exercised when distances and angles are compared between one structural determination and another, even when the esd's indicate that the differences are significant. This has been pointed out forcefully in two other recent publications on the structures of compounds related to those discussed here.[50,51] The discussion of the

---

[46] Cotton, F. A.; Duraj, S. A.; Extine, M. W.; Lewis, G. E.; Roth, W. J.; Schmulback, C. D.; Schwotzer, W. *J. Chem. Soc., Chem. Commun.* **1983**, 1377.

[47] Dean, P. A. W.; Vittal, J. J. *Can. J. Chem.* **1988**, *66*, 2443.

[48] Dean, P. A. W.; Vittal, J. J. In *Metal Binding in Sulfur-Containing Proteins*; Stillman, M. J., Shaw, C. F., Suzuki, K. T., Eds.; VCH Publishers, in press.

[49] Dance, I. G. *Polyhedron* **1986**, *5*, 1037.

[50] Rheingold, A. L.; Harper, J. R. *J. Organomet. Chem.* **1991**, *403*, 335.

Table V. Crystal and Refinement Data for 1 and the Salts of 2^+ and 3^+

	1	$\{2^+\}_2\{Zn_2Cl_6^{2-}\}$	$\{2^+\}_2\{Zn_6Cl_{14}^{2-}\}$	$\{3^+\}_2\{Zn_2Cl_6^{2-}\}$
molecular formula	$C_{20}H_{31}Cl_5Nb_2O_2$	$C_{66}H_{104}Cl_{12}Nb_6O_6Zn_2$	$C_{30}H_{45}Cl_{10}Nb_3O_3Zn_3$	$C_{60}H_{92}Cl_{14}Nb_6O_8Zn_2$
fw	666.54	2107.30	1283.09	2126.02
cryst system	orthorhombic	monoclinic	triclinic	monoclinic
space group	*F2dd*	*A2/m*	$P\bar{1}$	$P2_1/a$
a, Å	8.9028 (8)	14.7497 (8)	11.141 (4)	11.3770 (8)
b, Å	14.2570 (14)	16.3113 (18)	14.793 (7)	30.6303 (16)
c, Å	39.527 (4)	16.4104 (16)	14.792 (5)	11.4422 (9)
α, deg	90	90	74.14 (4)	90
β, deg	90	95.669 (6)	77.40 (3)	100.822 (6)
γ, deg	90	90	77.32 (4)	90
V, Å^3	5017.0 (9)	3928.8 (6)	2255 (1)	3916.5 (5)
Z	8	2[a]	2[b]	4[c]
D(calcd), Mg m^{-3}	1.76	1.78	1.89	1.80
μ(Mo Kα), cm^{-1}	14.3	18.8	19.2	20.0
temp, K	293	295	293	293
cryst size, mm	0.65 × 0.50 × 0.32	0.35 × 0.75 × 0.20	0.90 × 0.50 × 0.25	0.55 × 0.20 × 0.25
2θ limits, deg	2–50	2–50	2–50	2–50
no. of reflns for cell	25	25	22	25
2θ limits for cell, deg	40–50	40–50	40–50	40–50
no. of reflns collcd	1194	3909	8045	7619
no. of unique reflns	1170	3593	7951	6922
no. of obsd reflns	929	3289	4934	4391
criteria for observn	$I > 2.5\sigma(I)$	$I > 2.5\sigma(I)$	$I > 2.0\sigma(I)$	$I > 2.0\sigma(I)$
$R(F')$	0.057	0.040	0.104	0.071
$R_w(F')$	0.067	0.066	0.105	0.070
GoF	4.57	2.539	4.751	2.710
no. of refined params	132	153	475	257
max Δ/σ	0.81	0.27	4.91	0.16
max Δ, e Å^{-3}	0.79	0.84	1.81	1.17
N_o/N_v	7.0	21.5	10.4	17.1
K (weight modifier)	0.000 05	0.0005	0.0001	0.0001

[a] For $\{[(C_5Me_5)Nb(\mu\text{-}Cl)(\mu\text{-}O)]_3\}_2\{Zn_2Cl_6\}\cdot C_6H_{14}$. [b] For $\{[(\eta\text{-}C_5Me_5)Nb(\mu\text{-}Cl)(\mu\text{-}O)]_3\}\{Zn_3Cl_7\}$. [c] For $\{[(\eta\text{-}C_5Me_5)NbCl]_3(\mu\text{-}Cl)(\mu\text{-}O)_2(\mu_3\text{-}OH)(\mu_3\text{-}O)\}\{ZnCl_3\}$.

structure of 2^+ above, and the comparison of its structure with those of $\{[(\eta\text{-}C_5Me_5)Re(\mu\text{-}O)_2]_3\}^{2+}$ and $\{[(\eta\text{-}C_6Me_6)Nb(\mu\text{-}Cl)_2]_3\}^{n+}$, do not depend on the esd's of the individual determinations because the differences are very large (for example, 0.45 Å in the Nb–Nb distances).

Experimental Section

General Considerations. All manipulations were conducted using a standard double-manifold vacuum line, under argon or under vacuum. Samples were transferred in a dinitrogen-filled glovebag. Solvents were predried over molecular sieves and then distilled over $LiAlH_4$ (Et_2O, thf) or Na (toluene, hexane). Dichloromethane was refluxed over P_2O_5 before distillation. Water was distilled and deoxygenated by freeze–thaw methods. Zinc powder was dried under vacuum before use. The starting material $(\eta\text{-}C_5Me_5)_2NbCl_2$ was prepared by the literature method.[52] All other reagents were used as received.

Instruments used in this work were as follows: Varian XL-200 for ^1H, ^{13}C, and ^{93}Nb NMR spectra, with chemical shifts referenced to the nondeuterated solvent impurity or to $NbCl_5$; Perkin-Elmer 685 for infrared spectra, as KBr pellets or Nujol mulls; Kratos MS50 for mass spectra, using EI or FAB ionization; Faraday method with an Alpha Scientific magnet and Cahn electrobalance for magnetic moments at room temperature; Perkin-Elmer 330 for electronic spectra. Microanalyses (C, H, Cl) were performed by Beller Laboratorium, Göttingen, Germany, and molecular weights, by osmometry, by the Mikroanalytisches Laboratorium, Engelskirchen, Germany.

Oxidation of $(\eta\text{-}C_5Me_5)_2NbCl_2$: Preparation of $[(\eta\text{-}C_5Me_5)NbCl_2]_2(\mu\text{-}Cl)(\mu\text{-}OH)(\mu\text{-}O)$ (1). A solution of $(\eta\text{-}C_5Me_5)_2NbCl_2$ (2.0 g, 4.60 mmol) in thf (200 cm^3) containing one drop of water was incubated under O_2 (2.70 mmol), with stirring, at room temperature for 24 h. Over this period the color of the solution changed from dark brown to red-purple, and some orange-red precipitate formed. The solvent was removed under vacuum and the residue extracted with toluene (100 cm^3). Filtration gave a purple filtrate and an orange-red residue. This residue was washed with ether (50 cm^3) and dried under vacuum. Recrystallization from CH_2Cl_2/Et_2O gave 1 as an orange-red powder, yield 0.90 g (88%) (calculated according to eq 1). Crystals suitable for X-ray diffraction were obtained on setting aside a solution of 1 in CH_2Cl_2 which had been layered with Et_2O for 15 days. Anal. Calcd for $C_{20}H_{31}Nb_2Cl_5O_2$: C, 36.0; H, 4.6; Cl, 26.6. Found: C, 35.6; H, 4.5; Cl, 25.4. ^1H NMR spectrum (CH_2Cl_2-d_2 solution): 2.24, 2.20, 2.13 ppm (see also the Discussion and Figure 3). ^{93}Nb NMR spectrum ($CHCl_3$-*d* solution): −328.4 ppm. Infrared spectrum: 3500 cm^{-1} (weak, broad), ν(OH); 635, 590 cm^{-1} (strong), δ(Nb–O–Nb). See below for the characterization of 1 by X-ray crystallography.

Table VI. Atomic Coordinates and B_{iso} Values for 1

	x	*y*	*z*	B_{iso},[a] Å^2
Nb	0.41632	0.00079 (16)	0.03818 (3)	2.73 (8)
Cl(1)	0.1576 (6)	−0.0116 (4)	0.05674 (14)	5.2 (3)
Cl(2)	0.4719 (9)	−0.1504 (4)	0.06085 (15)	5.1 (3)
X(1)	0.5523 (16)	0	0	6.7 (8)
X(2)	0.3228 (13)	0.0875 (8)	0.0007 (3)	7.3 (6)
C(11)	0.507 (3)	0.1615 (16)	0.0534 (6)	5.5 (12)
C(12)	0.6247 (23)	0.1043 (20)	0.0539 (6)	5.1 (11)
C(13)	0.605 (3)	0.0427 (17)	0.0802 (8)	6.4 (14)
C(14)	0.456 (4)	0.0629 (24)	0.0957 (5)	7.6 (17)
C(15)	0.403 (4)	0.1384 (17)	0.0767 (7)	5.8 (14)
C(111)	0.495 (8)	0.2449 (22)	0.0341 (11)	23.5 (56)
C(121)	0.765 (3)	0.097 (3)	0.0321 (8)	10.2 (21)
C(131)	0.724 (5)	−0.0266 (24)	0.0950 (15)	18.8 (37)
C(141)	0.394 (8)	0.021 (3)	0.1265 (5)	14.7 (28)
C(151)	0.271 (5)	0.191 (3)	0.0855 (11)	12.3 (26)

[a] B_{iso} is the mean of the principal axes of the thermal ellipsoid.

Reduction of $[(\eta\text{-}C_5Me_5)NbCl_2]_2(\mu\text{-}Cl)(\mu\text{-}OH)(\mu\text{-}O)$ with Zinc: Preparation of $\{[(\eta\text{-}C_5Me_5)Nb(\mu\text{-}Cl)(\mu\text{-}O)]_3\}^+$ (2^+). A suspension of 1 (0.5 g, 0.75 mmol) in CH_2Cl_2 (100 cm^3) was stirred with zinc powder (0.40 g) for 24 h at room temperature. During this time the color of the solution changed from orange-red to

---

(51) Yoon, K.; Parkin, G.; Rheingold, A. L. *J. Am. Chem. Soc.* **1991**, *113*, 1437.

(52) Bunker, M. J.; de Cian, A.; Green, M. L. H. *J. Chem. Soc., Chem. Commun.* **1977**, 59.

Table VII. Atomic Coordinates and B_{iso} Values for $\{2^+\}_2\{Zn_2Cl_6{}^{2-}\}\bullet C_6H_{14}$

	x	y	z	B_{iso},[b] Å^2		x	y	z	B_{iso},[b] Å^2
Nb(1)	0.75086 (3)[a]	0	0.04373 (3)	1.815 (22)	C(23)	0.8386 (3)	0.7896 (3)	0.8435 (3)	2.57 (8)
Nb(2)	0.772169 (24)	−0.088188 (22)	−0.104885 (22)	1.765 (18)	C(231)	0.9377 (4)	0.7697 (4)	0.8621 (4)	4.00 (11)
Cl(1)	0.90542 (10)	0	−0.14016 (10)	2.57 (6)	C(24)	0.7683 (3)	0.7627 (3)	0.8906 (3)	2.79 (8)
Cl(2)	0.87927 (8)	0.09987 (7)	0.02582 (7)	2.64 (4)	C(241)	0.7784 (4)	0.7108 (4)	0.9653 (4)	4.73 (12)
O(1)	0.7127 (3)	0	−0.16838 (25)	2.03 (15)	C(25)	0.6840 (3)	0.7906 (3)	0.8500 (3)	2.85 (8)
O(2)	0.68993 (21)	−0.08781 (16)	−0.02024 (19)	2.08 (11)	C(251)	0.5918 (4)	0.7730 (4)	0.8759 (4)	4.69 (12)
C(11)	0.6331 (5)	0	0.1356 (4)	2.65 (11)	Zn	0.40344 (7)	0.5	0.03843 (5)	3.83 (4)
C(111)	0.5330 (6)	0	0.1058 (5)	4.01 (15)	Cl(11)	0.5	0.39485 (13)	0	5.24 (11)
C(12)	0.6865 (3)	0.0703 (3)	0.1554 (3)	2.72 (8)	Cl(12)	0.27145 (17)	0.5	−0.03833 (15)	5.23 (10)
C(121)	0.6550 (4)	0.1584 (4)	0.1477 (4)	4.22 (11)	Cl(13)	0.3948 (3)	0.5	0.17041 (17)	11.7 (3)
C(13)	0.7740 (3)	0.0434 (3)	0.1875 (3)	2.97 (8)	C(1001)[c]	0.0086 (21)	0.5	0.0951 (13)	4.8 (4)
C(131)	0.8487 (4)	0.0974 (4)	0.2243 (4)	4.48 (12)	C(1002)	0.045 (3)	0.5	0.003 (4)	15.6 (16)
C(21)	0.7018 (3)	0.8336 (3)	0.7782 (3)	2.74 (8)	C(1003)	−0.0083 (24)	0.4121 (16)	0.0226 (18)	5.1 (7)
C(211)	0.6344 (4)	0.8700 (4)	0.7157 (4)	4.31 (11)	C(1004)	−0.0006 (17)	0.4311 (15)	0.0587 (16)	2.8 (4)
C(22)	0.7982 (3)	0.8321 (3)	0.7738 (3)	2.77 (8)	C(1005)	0.0310 (20)	0.4655 (22)	0.0798 (17)	3.9 (5)
C(221)	0.8469 (4)	0.8645 (4)	0.7054 (4)	4.42 (11)	C(1006)	−0.0113 (18)	0.4600 (21)	0.0819 (16)	3.2 (4)

[a] Esd's refer to the last digit printed. [b] B_{iso} is the mean of the principal axes of the thermal ellipsoid. [c] The site occupancies of C(1001) and C(1002) are 0.50, and those of C(1003)–C(1006), 0.25.

Table VIII. Atomic Coordinates and B_{iso} Values for $\{2^+\}_2\{Zn_6Cl_{14}\}$[a]

	x	y	z	B_{iso},[b] Å^2		x	y	z	B_{iso},[b] Å^2
Nb(1)	0.79993 (16)	0.78422 (12)	0.12386 (12)	3.72 (8)	C(24A)	0.952 (5)	0.579 (4)	0.386 (3)	4.6 (10)
Nb(2)	0.79999 (16)	0.62413 (12)	0.28400 (12)	3.73 (9)	C(241A)	0.973 (4)	0.695 (3)	0.411 (3)	4.9 (9)
Nb(3)	0.69142 (16)	0.62716 (12)	0.12729 (13)	3.92 (9)	C(25)	0.9803 (25)	0.5402 (22)	0.3608 (19)	0.8 (5)
Cl(1)	0.6937 (5)	0.7900 (4)	0.2895 (4)	5.4 (3)	C(251)	1.101 (3)	0.5550 (22)	0.3163 (21)	2.6 (6)
Cl(2)	0.5818 (7)	0.6157 (5)	0.2928 (5)	9.0 (5)	C(25A)	0.924 (5)	0.491 (3)	0.372 (3)	3.8 (9)
Cl(3)	0.5815 (7)	0.7935 (5)	0.1175 (5)	8.8 (4)	C(251A)	1.048 (13)	0.476 (10)	0.312 (9)	27.4 (48)
O(2)	0.8127 (11)	0.7017 (8)	0.0430 (9)	4.8 (7)	C(31)	0.516 (4)	0.577 (4)	0.092 (4)	3.4 (9)
O(3)	0.9178 (10)	0.7000 (8)	0.1997 (8)	3.9 (6)	C(311)	0.390 (5)	0.614 (4)	0.131 (4)	7.7 (13)
O(1)	0.8123 (11)	0.5439 (8)	0.2009 (9)	4.6 (7)	C(31A)	0.536 (5)	0.604 (4)	0.045 (5)	4.3 (10)
C(11)	0.781 (5)	0.937 (4)	0.005 (4)	3.1 (9)	C(311A)	0.450 (6)	0.714 (5)	−0.021 (5)	11.4 (19)
C(111)	0.677 (4)	0.979 (3)	−0.042 (3)	5.5 (10)	C(32)	0.576 (6)	0.638 (4)	−0.003 (4)	5.1 (12)
C(11A)	0.837 (8)	0.907 (5)	−0.018 (4)	4.8 (12)	C(321)	0.565 (5)	0.713 (3)	−0.085 (4)	6.7 (11)
C(111A)	0.885 (7)	0.865 (5)	−0.114 (5)	11.5 (22)	C(32A)	0.637 (8)	0.606 (5)	−0.016 (4)	5.2 (13)
C(12)	0.900 (5)	0.873 (3)	−0.029 (3)	2.4 (7)	C(321A)	0.678 (5)	0.677 (4)	−0.118 (4)	8.3 (13)
C(121)	0.954 (5)	0.830 (4)	−0.107 (4)	6.2 (12)	C(33)	0.692 (10)	0.585 (7)	−0.023 (6)	9.5 (30)
C(12A)	0.936 (7)	0.869 (4)	0.005 (5)	6.0 (14)	C(331)	0.814 (6)	0.584 (4)	−0.094 (4)	9.5 (16)
C(121A)	1.066 (13)	0.806 (9)	−0.018 (9)	23.4 (53)	C(33A)	0.726 (4)	0.540 (5)	0.002 (4)	3.6 (9)
C(13)	0.983 (3)	0.8623 (22)	0.042 (3)	1.5 (6)	C(331A)	0.855 (5)	0.474 (4)	−0.017 (4)	9.3 (15)
C(131)	1.106 (5)	0.816 (3)	0.028 (4)	5.3 (11)	C(34)	0.723 (4)	0.501 (4)	0.044 (5)	3.3 (8)
C(13A)	0.955 (5)	0.876 (4)	0.083 (4)	4.4 (11)	C(341)	0.813 (6)	0.412 (4)	0.083 (4)	9.8 (16)
C(131A)	1.102 (5)	0.818 (4)	0.078 (4)	6.4 (14)	C(34A)	0.675 (7)	0.478 (3)	0.092 (5)	4.9 (11)
C(14)	0.907 (3)	0.9148 (24)	0.1148 (20)	0.9 (5)	C(341A)	0.683 (6)	0.385 (4)	0.172 (4)	9.0 (15)
C(141)	0.970 (4)	0.913 (3)	0.195 (3)	5.0 (10)	C(35)	0.614 (8)	0.489 (4)	0.124 (4)	4.7 (11)
C(14A)	0.830 (6)	0.950 (3)	0.101 (3)	4.4 (11)	C(351)	0.568 (5)	0.420 (3)	0.215 (3)	6.6 (11)
C(141A)	0.893 (7)	0.942 (5)	0.196 (5)	12.0 (21)	C(35A)	0.550 (7)	0.521 (6)	0.122 (4)	5.6 (12)
C(15)	0.775 (5)	0.955 (3)	0.094 (3)	3.2 (9)	C(351A)	0.434 (7)	0.514 (5)	0.201 (5)	12.9 (21)
C(151)	0.706 (4)	1.016 (3)	0.157 (3)	6.0 (11)	Zn(1)	0.2856 (3)	−0.13654 (22)	0.36348 (22)	7.01 (18)
C(15A)	0.769 (6)	0.955 (4)	0.041 (7)	6.9 (19)	Zn(2)	0.3421 (3)	0.0967 (3)	0.3776 (3)	9.37 (24)
C(151A)	0.671 (5)	1.011 (4)	0.110 (4)	8.1 (15)	Zn(3)	0.6575 (3)	0.1224 (3)	0.4038 (3)	9.31 (23)
C(21)	0.913 (7)	0.409 (6)	0.356 (5)	13.1 (19)	Zn(4)	−0.0003 (4)	0.0658 (4)	0.4335 (4)	5.7 (3)
C(211)	0.950 (4)	0.378 (3)	0.329 (3)	6.3 (9)	Cl(101)	0.3902 (7)	−0.0143 (5)	0.2896 (5)	9.0 (5)
C(21A)	0.875 (5)	0.473 (3)	0.389 (3)	2.8 (8)	Cl(102)	0.6109 (7)	0.2093 (5)	0.5133 (6)	9.2 (5)
C(211A)	0.714 (5)	0.419 (4)	0.440 (4)	8.4 (14)	Cl(103)	0.0834 (6)	−0.0797 (6)	0.4193 (6)	9.4 (5)
C(22)	0.809 (6)	0.492 (4)	0.425 (4)	4.3 (11)	Cl(104)	0.3275 (8)	0.0378 (5)	0.5375 (5)	9.8 (5)
C(221)	0.670 (4)	0.463 (3)	0.487 (3)	5.4 (10)	Cl(105A)	0.5361 (15)	0.1649 (14)	0.3070 (13)	6.5 (10)
C(22A)	0.777 (4)	0.522 (5)	0.445 (3)	2.9 (11)	Cl(105B)	0.4639 (15)	0.1927 (14)	0.3370 (15)	7.1 (10)
C(221A)	0.653 (10)	0.564 (8)	0.509 (7)	18.6 (35)	Cl(106A)	0.1439 (13)	0.1629 (10)	0.3715 (12)	7.3 (9)
C(23)	0.778 (4)	0.578 (4)	0.457 (3)	2.6 (8)	Cl(106B)	0.1949 (21)	0.2203 (19)	0.3203 (13)	16.2 (17)
C(231)	0.685 (5)	0.630 (4)	0.516 (4)	6.3 (11)	Cl(107A)	0.8555 (13)	0.1294 (12)	0.3374 (10)	7.1 (9)
C(23A)	0.817 (5)	0.608 (3)	0.450 (3)	3.5 (10)	Cl(107B)	0.8044 (21)	0.1794 (12)	0.2796 (17)	14.0 (15)
C(231A)	0.733 (8)	0.676 (6)	0.505 (5)	12.8 (23)	Cl(108A)	0.321 (5)	−0.258 (5)	0.305 (5)	9.4 (32)
C(24)	0.904 (3)	0.6182 (20)	0.4140 (21)	0.8 (5)	Cl(108B)	0.310 (4)	−0.1979 (24)	0.243 (3)	7.1 (18)
C(241)	0.895 (6)	0.701 (5)	0.443 (5)	10.9 (19)	Cl(108C)	0.275 (7)	−0.235 (5)	0.281 (6)	8.4 (34)

[a] The site occupancies of all C atoms, of Cl(105A)–Cl(107B), and of Zn(4) were 0.5, and those of Cl(108A)–Cl(108C) were 0.33. [b] B_{iso} is the mean of the principal axes of the thermal ellipsoid.

brown and then to deep green. The mixture was filtered and the filtrate reduced to a volume of 30 cm^3. The solution was layered with hexane (30 cm^3). On setting aside the solution for 48 h at room temperature, a crop of green crystals formed (0.52 g). Recrystallization of these from CH_2Cl_2/Et_2O gave the salt $\{[(\eta\text{-}C_5Me_5)Nb(\mu\text{-}Cl)(\mu\text{-}O)]_3\}^+\{[(\eta\text{-}C_5Me_5)Nb]_3(\mu\text{-}Cl)_2(\mu\text{-}OH)(\mu\text{-}O)_3\}^+\{Zn_4Cl_{10}\}^{2-}$ (0.48 g). Recrystallization from CH_2Cl_2/hexane gave the salt $\{2^+\}_2\{Zn_2Cl_6\}^{2-}$ (0.36 g). The salt $\{2^+\}_2\{Zn_6Cl_{14}\}^{2-}$ was also obtained from CH_2Cl_2/hexane. Microanalysis of the material obtained from CH_2Cl_2/Et_2O gave the following (%): C, 31.4; H, 4.2; Cl, 22.1. The compound was shown to be $\{2\}\{[(\eta\text{-}C_5Me_5)Nb]_3(\mu\text{-}Cl)_2(\mu\text{-}OH)(\mu\text{-}O)_3\}\{Zn_4Cl_{10}\}\cdot 0.5(C_2H_5)_2O\cdot 0.5CH_2Cl_2$ by X-ray crystallography. This requires the following (%): C, 31.9; H, 4.2; Cl, 24.1. The material from CH_2Cl_2/hexane analyzed as (%) C, 33.6; H, 5.1; Cl, 20.0. This was shown by X-ray crystallography to be $\{2\}_2Zn_2Cl_6{\cdot}C_6H_{14}$, which requires (%) C, 37.6; H, 5.0; Cl, 20.2. The $\{2^+\}_2\{Zn_6Cl_{14}\}^{2-}$ salt was obtained in insufficient quantity for microanalysis. It would require (%) C, 28.1; H, 3.5; Cl, 27.6.

The mass spectrum (FAB mode) of the $Zn_2Cl_6^{2-}$ salt showed a peak at m/e = 837 (2^+, calculated for $^{35}Cl_3$) and at 820 (2^+ − OH). All of the salts showed a single resonance in the ^1H NMR spectrum (CH_2Cl_2-d_2 solution) at 2.10 ppm, accompanied by a number of weak signals in the same region (see Discussion). All the salts showed an absorption band at 570 cm^{-1} in the infrared spectrum. This was assigned to a composite vibration of the $[Nb(\mu\text{-}Cl)(\mu\text{-}O)]_3$ core.

Oxidation of 2^+ with O_2: Preparation of $\{[(\eta\text{-}C_5Me_5)NbCl]_3(\mu\text{-}Cl)(\mu\text{-}O)_2(\mu_3\text{-}OH)(\mu_3\text{-}O)\}^+$ (3^+) as the $\{3^+\}_2\{Zn_2Cl_6^{2-}\}$ Salt. A solution of $\{2^+\}_2\{Zn_2Cl_6^{2-}\}$ (0.5 g) in CH_2Cl_2 (100 cm^3) was incubated with O_2 (1 atm) at room temperature for 18 h. The color of the solution changed from green to yellow over this period. The volume was reduced to 50 cm^3 under vacuum, and ether (50 cm^3) was layered onto the solution. Orange-red crystals formed over 24 h. These were collected by filtration, washed with ether (30 cm^3), and dried under vacuum. Yield: 0.37 g, 70%. Anal. Found: C, 33.9; H, 4.3; Cl, 23.4. Calcd for $C_{60}H_{92}Cl_{14}Nb_6O_8Zn_2$ ($\{3^+\}_2\{Zn_2Cl_6\}^{2-}$): C, 33.7; H, 4.2; Cl, 24.2. Mass spectrum (FAB): m/e = 889 ($\{3\}^+$), 854 ($\{3 - Cl\}^+$), and 719 ($\{3 - Cl - C_5Me_5\}^+$). ^1H NMR (liquid-SO_2 solution): 2.25, 2.18 ppm in 2:1 relative ratio, assigned to $C_5(CH_3)_5$ attached to Nb(2), Nb(3), and Nb(1), respectively (see Figure 10 for the numbering scheme). ^{13}C NMR (SO_2 solution): 135.7, 134.1 ppm ($C_5(CH_3)_5$) and 13.0, 12.0 ppm ($C_5(CH_3)_5$). Infrared spectrum: 3300–3400 cm^{-1} (broad, weak), ν(OH). The compound was also characterized by X-ray diffraction (see below).

Reduction of $\{3^+\}_2\{Zn_2Cl_6^{2-}\}$ with Zinc: Formation of $\{2^+\}_2\{Zn_2Cl_6^{2-}\}$. A solution of $\{3^+\}_2\{Zn_2Cl_6\}$ (0.50 g, 0.23 mmol) in CH_2Cl_2 (100 cm^3) was stirred with zinc powder (0.40 g) at room temperature for 3 days. During this time the color of the solution changed from orange-yellow to green. Filtration of the mixture gave a green filtrate, which was reduced to 50 cm^3 under vacuum. On layering of the solution with hexane (30 cm^3) and setting it aside for 24 h, an oily green precipitate was obtained. Recrystallization from CH_2Cl_2 (20 cm^3)/hexane (10 cm^3)/ether (10 cm^3) gave crystalline $\{2^+\}_2\{Zn_2Cl_6^{2-}\}$ (0.35 g, 74%). ^1H NMR (CH_2Cl_2-d_2 solution): 2.10 ppm. The compound was conclusively identified by comparison of the cell dimensions and space group with those of an authentic sample (Table V).

X-ray Crystallography. X-ray diffraction experiments were carried out on an Enraf-Nonius CAD-4 diffractometer operating under control of the NRCCAD software.[53] The radiation was Mo Kα, λ = 0.710 73 Å. Data were collected using the $\omega/2\theta$ scan method. Refinement used the NRCVAX suite of programs.[54] The weighting scheme was of the form $w = 1/(\sigma(F)^2 + kF^2)$. Scattering factors for the neutral atoms, corrected for the real and imaginary parts of the anomalous dispersion, were taken from ref 55. Crystal and refinement data for 1, the $Zn_2Cl_6^{2-}$ and $Zn_6Cl_{14}^{2-}$ salts of 2^+, and the $Zn_2Cl_6^{2-}$ salt of 3^+ are collected in Table V. In the final refinements, hydrogen atoms were included as fixed contributors with C–H = 0.96 Å and an isotropic B equal to that of the carbon atom to which they were attached.

The structure of $\{2^+\}_2\{Zn_4Cl_{10}^{2-}\}$ was published previously.[26] The most accurate determination of the structure of 2^+ was for the $Zn_2Cl_6^{2-}$ salt, which is discussed here. The coordinates of the $Zn_4Cl_{10}^{2-}$ salt are available as supplementary material to ref 26.

Structure Determination of 1. As noted above, the structure of 1 was refined previously in the monoclinic space group Cc.[26] During that work weak reflections interleaved on the c axis suggested that the true dimension might be ca. 40 rather than 20 Å. The crystals were small and of poor quality, and the weak reflections could not be reproducibly observed. Recently we obtained a large, well-formed, crystal of 1, for which the weak reflections were clearly identifiable. Redetermination of the crystal data showed that the correct space group was the orthorhombic $F2dd$ (see Table V). Structure solution and refinement were uneventful. The bridging Cl, OH, and O groups were disordered, due to the presence of the isomers discussed above. The Cl and O atoms were all defined as chlorine atoms with a site occupancy of 0.65. They are listed as X(1) and X(2) in Table VI, which gives the coordinates. The new refinement gave distances and angles similar to those reported previously.[26] Details are available as supplementary material to the present paper.

Table IX. Atomic Coordinates and B_{iso} Values for $\{3^+\}_2\{Zn_2Cl_6^{2-}\}$

	x	y	z	B_{iso},[a] Å^2
Nb(1)	0.67616 (11)[b]	0.39004 (4)	0.44962 (11)	1.95 (6)
Nb(2)	0.55397 (11)	0.33752 (4)	0.61540 (11)	2.09 (5)
Nb(3)	0.44359 (11)	0.34801 (4)	0.32707 (11)	1.98 (5)
Cl(1)	0.6393 (3)	0.46329 (11)	0.4876 (3)	3.45 (19)
Cl(2)	0.6331 (3)	0.26502 (12)	0.6478 (3)	3.42 (18)
Cl(3)	0.4788 (3)	0.28239 (12)	0.2247 (3)	3.35 (17)
Cl(4)	0.3666 (3)	0.30036 (12)	0.4837 (3)	2.92 (16)
O(1)	0.4918 (7)	0.3813 (3)	0.4857 (7)	2.0 (4)
O(2)	0.6032 (7)	0.3222 (3)	0.4428 (7)	2.1 (4)
O(3)	0.6968 (7)	0.3693 (3)	0.6155 (7)	2.5 (4)
O(4)	0.5737 (7)	0.3824 (3)	0.2934 (7)	2.1 (4)
C(11)	0.8571 (12)	0.4261 (4)	0.4011 (11)	2.4 (3)
C(12)	0.8155 (13)	0.3970 (5)	0.3090 (12)	3.2 (3)
C(13)	0.8250 (13)	0.3554 (5)	0.3584 (12)	3.1 (3)
C(14)	0.8746 (13)	0.3589 (5)	0.4789 (13)	3.4 (3)
C(15)	0.8927 (12)	0.4022 (5)	0.5098 (12)	2.6 (3)
C(111)	0.8722 (14)	0.4731 (5)	0.3841 (13)	3.9 (3)
C(121)	0.7758 (15)	0.4084 (5)	0.1798 (14)	4.4 (4)
C(131)	0.7993 (15)	0.3131 (6)	0.2878 (14)	4.7 (4)
C(141)	0.9075 (16)	0.3222 (6)	0.5652 (16)	5.6 (4)
C(151)	0.9422 (14)	0.4217 (5)	0.6268 (13)	4.0 (3)
C(21)	0.5862 (13)	0.3376 (5)	0.8327 (13)	3.4 (3)
C(22)	0.5869 (13)	0.3815 (5)	0.7998 (12)	3.2 (3)
C(23)	0.4703 (12)	0.3916 (5)	0.7364 (12)	2.9 (3)
C(24)	0.3998 (12)	0.3535 (4)	0.7355 (11)	2.5 (3)
C(25)	0.4729 (13)	0.3187 (5)	0.7918 (13)	3.4 (3)
C(211)	0.6914 (15)	0.3132 (6)	0.9082 (14)	4.8 (4)
C(221)	0.6871 (14)	0.4133 (5)	0.8309 (13)	4.2 (4)
C(231)	0.4283 (14)	0.4369 (5)	0.6939 (13)	4.1 (3)
C(241)	0.2660 (14)	0.3526 (5)	0.6955 (13)	4.0 (3)
C(251)	0.4328 (15)	0.2750 (6)	0.8198 (14)	4.7 (4)
C(31)	0.3444 (13)	0.4120 (5)	0.2184 (12)	3.2 (3)
C(32)	0.3427 (12)	0.3778 (4)	0.1375 (12)	2.7 (3)
C(33)	0.2653 (12)	0.3435 (5)	0.1673 (12)	3.0 (3)
C(34)	0.2222 (13)	0.3597 (5)	0.2686 (13)	3.4 (3)
C(35)	0.2741 (12)	0.3988 (4)	0.3025 (11)	2.5 (3)
C(311)	0.4057 (15)	0.4536 (6)	0.2154 (14)	4.8 (4)
C(321)	0.4008 (17)	0.3743 (6)	0.0327 (16)	6.0 (5)
C(331)	0.2190 (17)	0.3058 (7)	0.0930 (16)	6.4 (5)
C(341)	0.1269 (19)	0.3379 (7)	0.3248 (18)	7.8 (6)
C(351)	0.2436 (16)	0.4300 (6)	0.3976 (15)	5.6 (4)
Zn	0.07073 (18)	0.45741 (7)	0.96208 (17)	4.50 (10)
Cl(11)	0.0782 (4)	0.49557 (16)	1.1417 (4)	4.98 (22)
Cl(12)	0.2369 (5)	0.46733 (21)	0.8960 (5)	8.4 (3)
Cl(13)	0.0105 (5)	0.38976 (17)	0.9720 (5)	7.9 (3)

[a] B_{iso} is the mean of the principal axes of the thermal ellipsoid. [b] Esd's (in parentheses) refer to the last digit printed.

Structure Determination of the $Zn_2Cl_6^{2-}$ Salt of 2^+. This was uneventful, except in the very last stages. It was found that the crystal contained a molecule of hexane as solvent of crystallization. This molecule was very severely disordered, almost forming a sphere of electron density. In the final refinement, the $C_5(CH_3)_5$ carbon atoms were refined isotropically. Anisotropic refinement did not improve the R value nor indicate markedly nonspherical thermal ellipsoids. All the major residual peaks in a difference Fourier synthesis were located in the region of the hexane molecule. The coordinates are given in Table VII, diagrams in Figures 4 and 5, and relevant distances and angles in Tables II and IV, and other details are available as supplementary material.

Structure Determination of the $Zn_6Cl_{14}^{2-}$ Salt of 2^+. The solution of the structure was routine. However the refinement posed major problems. The least of these was disorder in all three of the η-$C_5(CH_3)_5$ rings. The most serious was the chlorozincate

---

[53] Le Page, Y.; White, P. S.; Gabe, E. J. Annual Meeting of the American Crystallographic Association, Hamilton, Ontario, Canada, 1986.

[54] Gabe, E. J.; LePage, Y.; Charland, J. P.; Lee, F. L.; White, P. S. *J. Appl. Crystallogr.* **1989**, *22*, 384.

[55] *International Tables for X-ray Crystallography*; Kynoch Press: Birmingham, England, 1974; Vol. IV.

anion. This formed an infinite chain running through the cell. Although the structure can be described as repeating units of $Zn_6Cl_{14}^{2-}$, with the structure shown in Figure 7, the chain was disordered at all sites. It appeared that the chains actually consisted of a mixture of $[Zn_6Cl_{14}^{2-}]_n$ and $[Zn_7Cl_{16}^{2-}]_n$, the latter containing an adamantane-like $Zn_4(\mu\text{-}Cl)_6^{2+}$ unit. The objective of the present work was the characterization of the $\{[(\eta\text{-}C_5Me_5)Nb(\mu\text{-}Cl)(\mu\text{-}O)]_3\}^+$ cation, and it was clear that only a very complicated and carefully refined model for the chlorozincate anion would be adequate to describe the salt. No detailed investigation of the site occupancies of the Zn and Cl atoms was undertaken. In the final difference Fourier all of the largest peaks were in the region of the chlorozincate chain. The atomic coordinates are given in Table VIII, diagrams in Figures 4 and 7, and relevant distances and angles in Table II, and other details are available as supplementary material.

Structure Determination of the $Zn_2Cl_6^{2-}$ Salt of 3^+. This was uneventful. Some of the C atoms had nonpositive thermal parameters when refined anisotropically. This was due to the low percentage of observed data. There was also evidence of disorder in the $C_5(CH_3)_5$ ring attached to Nb(3). Because of the limited data, no attempt was made to model this disorder, and all C atoms were refined isotropically. The atomic coordinates are given in Table IX, diagrams in Figures 8 and 10 (the $Zn_2Cl_6^{2-}$ anion was similar to that shown in Figure 5, as is clear from Table IV), and relevant distances and angles in Tables III and IV. Other details are available as supplementary material.

Acknowledgment. We thank Daniel F. Drummond for assistance with the mass spectra and with the X-ray programs and Prof. Philip Dean (Western Ontario) for helpful discussions on the structures of chlorozincate anions. The Natural Sciences and Engineering Research Council of Canada and the Petroleum Research Fund, administered by the American Chemical Society, are acknowledged for their financial support. S.K. thanks the Karadeniz Technical University for study leave.

Registry No. 1a, 137172-82-8; **1b**, 133601-68-0; $\{2^+\}_2\{Zn_2Cl_6\}^{2-}$, 137328-38-2; $\{2^+\}_2\{Zn_6Cl_{14}\}^{2-}$, 137328-39-3; $\{2\}\{[(\eta\text{-}C_5Me_5)Nb]_3(\mu\text{-}Cl)_2(\mu\text{-}OH)(\mu\text{-}O)_3\}\{Zn_4Cl_{10}\}\cdot 0.5(C_2H_5)_2O\cdot 0.5CH_2Cl_2$, 133624-65-4; $\{3^+\}_2\{Zn_2Cl_6^{2-}\}$, 137115-60-7; $\{[(\eta\text{-}C_5Me_5)Nb(\mu\text{-}Cl)(\mu\text{-}O)]_3\}^+\{[(\eta\text{-}C_5Me_5)Nb]_3(\mu\text{-}Cl)_2(\mu\text{-}OH)(\mu\text{-}O)_3\}^+\{Zn_4Cl_{10}\}^{2-}$, 133624-64-3; $(\eta\text{-}C_5Me_5)_2NbCl_2$, 95313-61-4.

Supplementary Material Available: Figures showing full numbering schemes and tables of hydrogen atom positions, anisotropic and isotropic thermal parameters, and comprehensive distances and angles for 1, $\{2^+\}_2\{Zn_2Cl_6^{2-}\}$, $\{2^+\}_2\{Zn_6Cl_{14}^{2-}\}$, and $\{3^+\}_2\{Zn_2Cl_6^{2-}\}$ (36 pages); tables of $|F_o|$ and $|F_c|$ values for the same four complexes (70 pages). Ordering information is given on any current masthead page.

Interaction of Alkylaluminum Reagents with Organotransition-Metal Arene Complexes: Net Addition of Alkide, Haloalkide, and Dichloromethide to $[(arene)_2Fe]^{2+}$ Cations

Jerry L. Atwood,[1a] Sean D. Christie,[1b] Michael D. Clerk,[1b] David A. Osmond,[1b] K. Craig Sturge,[1b] and Michael J. Zaworotko*,[1b]

Departments of Chemistry, Saint Mary's University, Halifax, Nova Scotia B3H 3C3, Canada, and University of Alabama, University, Alabama 35487

Received June 24, 1991

$AlEt_3$ reacts with the hexafluorophosphate salts of Ar_2Fe^{2+} cations (Ar = arene = benzene (**1a**), *p*-xylene (**1b**), mesitylene (**1c**), pentamethylbenzene (**1d**), hexamethylbenzene (**1e**)) in dichloromethane or 1,2-dichloroethane to afford $ChArFe^+$ (Ch = cyclohexadienyl) cations. The major products, the hexafluorophosphate salts of **2a–e**, result from net Et^- addition to a single arene ring. The corresponding reactions with $AlMe_3$ in CH_2X_2 (X = Cl, Br) are more complex and afford characterizable products for **1c**,**e** only. The unexpected major products of these reactions are the hexafluorophosphate salts of the $[(6\text{-}CH_2X\text{-}Ch)ArFe]^+$ monocations **3c**,**e** (X = Cl) and **4c**,**e** (X = Br), derived from net addition of CH_2X, rather than the expected methide addition products, **5a–e**. **1c** reacts with $[N(CH_2CH_2O)_3Al_2Me_3]_2$ (**6**), a compound that contains an octahedral aluminum methyl moiety, in dichloromethane to produce yet another $ChArFe^+$ species, (η^5-*exo*-6-(dichloromethyl)-1,3,5-trimethylcyclohexadienyl)(η^6-mesitylene)iron(II) hexafluorophosphonate (**7c**[PF_6]), which is the result of net addition of $CHCl_2^-$. The methide addition monocationic product **5c**[PF_6] can be prepared in low yield from $AlMe_3$ or **6** and **1c** if benzene and 1,2-dichloroethane, respectively, are utilized as solvent. The relevance of these reactions is discussed in the general context of transition-metal activation of Ar molecules. In addition to spectroscopic characterization, several compounds were characterized by X-ray crystallography. Full crystallographic details of the CH_2Cl-Ch and $CHCl_2$-Ch cations **3c** and **7c**, respectively, are presented and discussed in the context of related ChFe compounds: **3c**[PF_6], orthorhombic, *Pcab*, with $a = 15.2496$ (9) Å, $b = 15.5537$ (10) Å, $c = 17.5146$ (16) Å, $Z = 8$, $R = 0.059$, $R_w = 0.058$ for 2506 independent, observed ($I > 2.5\sigma(I)$), and absorption-corrected reflections; **7c**[PF_6]$\cdot(CH_3)_2CO$, monoclinic, $P2_1/c$, with $a = 18.762$ (3) Å, $b = 8.758$ (2) Å, $c = 17.104$ (3) Å, $\beta = 113.40$ (2)°, $Z = 4$, $R = 0.049$, $R_w = 0.055$ for 2051 independent, observed ($I > 2.5\sigma(I)$), and absorption-corrected reflections.

Introduction

Alkylaluminum reagents have found widespread application as stoichiometric carbanion sources in organic chemistry,[2] in particular toward the carbonyl moiety, for which they have been found to be capable of selective reduction.[2,3] However, their adoption in organo-

---

(1) (a) University of Alabama. (b) Saint Mary's University.

(2) Zietz, J. R., Jr.; Robinson, G. C.; Lindsay, K. L. In *Comprehensive Organometallic Chemistry*; Wilkinson, G., Stone, F. G. A., A., Abel, E. W., Eds.; Pergamon Press: Oxford, England, 1983; Vol. 6, Chapter 46, p 365.

0276-7333/92/2311-0337$03.00/0